

**AD748583**

Technical Report

**R 773**



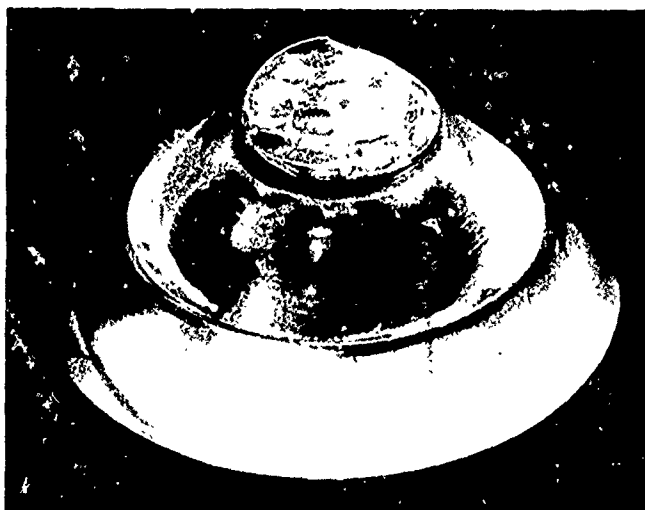
NAVAL CIVIL ENGINEERING LABORATORY

Port Hueneme, California 93043

Sponsored by

NAVAL FACILITIES ENGINEERING COMMAND

August 1972



*SEE AD746594*

**WINDOWS FOR EXTERNAL OR INTERNAL HYDROSTATIC**

**PRESSURE VESSELS—PART VII. Effect of Temperature and**

**Flange Configurations on Critical Pressure of 90-Degree Conical**

**Acrylic Windows Under Short-Term Loading**

Approved for public release; distribution unlimited.

Reproduced by  
**NATIONAL TECHNICAL  
INFORMATION SERVICE**  
U.S. Department of Commerce  
Springfield VA 22151

D D C  
REF ID: A6594  
SEP 21 1972  
RECORDED  
C  
55

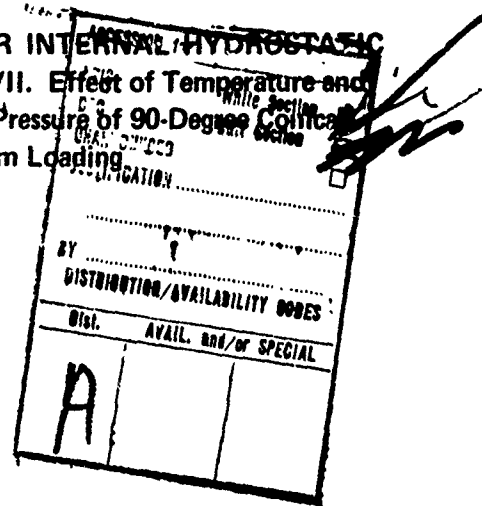
~~WINDOWS FOR EXTERNAL OR INTERNAL HYDROSTATIC  
PRESSURE VESSELS—PART VII. Effect of Temperature and  
Flange Configurations on Critical Pressure of 90-Degree Conical  
Acrylic Windows Under Short-Term Loading~~

Technical Report R-773

YF 51.543.008.01.001

by

J. D. Stachiw and J. R. McKay



## ABSTRACT

Conical acrylic windows of 90-degree included angle and 0.083 to 0.775 thickness-to-minor-diameter ( $t/D$ ) ratios have been tested to ultimate failure under short-term hydrostatic loading. The ambient temperature was varied from 32°F to 90°F and the relationship between minor window diameter ( $D$ ) and minor window cavity diameter in the flange ( $D_f$ ) varied from 0.970 to 1.500. The test results show that the critical pressure of identical windows at 90°F is approximately 10% to 20% less than at 70°F, and at 32°F it is approximately 15% to 25% more than at 70°F. The increase in critical pressure of windows with identical  $t/D$  ratios due to changes in  $D/D_f$  ratio is as large as 100% from the critical pressures associated with the standard  $D/D_f = 1.000$  ratio. As a rule, an increase in  $D/D_f$  ratio raised the critical pressure of windows with  $t/D \geq 0.375$  significantly, while for windows with  $t/D < 0.375$ , it had no effect or very little. To improve the critical pressure of 90-degree conical acrylic windows, it is recommended that such windows be designed with a window/flange mismatch ratio of  $D/D_f > 1.00$ , the exact magnitude depending on the window's  $t/D$  ratio, service, and design considerations.

Approved for public release; distribution unlimited.

Copies available at the National Technical Information Service  
(NTIS), Sills Building, 5285 Port Royal Road, Springfield, Va. 22151

Unclassified

Security Classification

DOCUMENT CONTROL DATA - R & D

(Security classification of title, body of abstract and indexing annotation must be entered when the overall report is classified)

1. ORIGINATING ACTIVITY (Corporate author) Naval Civil Engineering Laboratory Port Hueneme, California 93043		2a. REPORT SECURITY CLASSIFICATION Unclassified
2b. GROUP		
3. REPORT TITLE WINDOWS FOR EXTERNAL OR INTERNAL HYDROSTATIC PRESSURE VESSELS—PART VII. Effect of Temperature and Flange Configurations on Critical Pressure of 90-Degree Conical Acrylic Windows Under Short-Term Loading		
4. DESCRIPTIVE NOTES (Type of report and inclusive dates) Final; June 1969—June 1970		
5. AUTHOR(S) (First name, middle initial, last name) J. D. Stachiw and J. R. McKay		
6. REPORT DATE August 1972	7a. TOTAL NO. OF PAGES 51	7b. NO. OF REFS 14
8a. CONTRACT OR GRANT NO.		
8b. PROJECT NO. YF 51.543.008.01.001		
8c.		
8d.		
9b. OTHER REPORT NO(S) (Any other numbers that may be assigned this report) TR-773		
10. DISTRIBUTION STATEMENT Approved for public release; distribution unlimited.		
11. SUPPLEMENTARY NOTES	12. SPONSORING MILITARY ACTIVITY Naval Facilities Engineering Command Washington, D. C. 20390	
13. ABSTRACT Conical acrylic windows of 90-degree included angle and 0.083 to 0.775 thickness-to-minor-diameter ( $t/D$ ) ratios have been tested to ultimate failure under short-term hydrostatic loading. The ambient temperature was varied from 32°F to 30°F and the relationship between minor window diameter ( $D$ ) and minor window cavity diameter in the flange ( $D_f$ ) varied from 0.970 to 1.500. The test results show that the critical pressure of identical windows at 90°F is approximately 10% to 20% less than at 70°F, and at 32°F it is approximately 15% to 25% more than at 70°F. The increase in critical pressure of windows with identical $t/D$ ratios due to changes in $D/D_f$ ratio is as large as 100% from the critical pressures associated with the standard $D/D_f = 1.000$ ratio. As a rule, an increase in $D/D_f$ ratio raised the critical pressure of windows with $t/D \geq 0.375$ significantly, while for windows with $t/D < 0.375$ , it had no effect or very little. To improve the critical pressure of 90-degree conical acrylic windows, it is recommended that such windows be designed with a window/flange mismatch ratio of $D/D_f > 1.00$ , the exact magnitude depending on the window's $t/D$ ratio, service, and design considerations.		
<p style="text-align: center;">Details of illustrations in this document may be better seen on microfiche</p>		

DD FORM 1 NOV 68 1473 (PAGE 1)

S/N 0101-807-6601

Unclassified  
Security Classification

**Unclassified**

Security Classification

14 KEY WORDS	LINK A		LINK B		LINK C	
	ROLE	WT	ROLE	WT	ROLE	WT
Pressure vessel windows						
Acrylic plastic						
Conical windows						
Short-term pressurization						
Long-term pressurization						
Failure modes						
Displacement						
Deformation						
Fracture patterns						
Window frame designs						
Submersible windows						
Undersea habitat windows						
Deep-submergence windows						
Viewports						
Hyperbaric chamber windows						

DD FORM 1 NOV 68 1473 (BACK)  
(PAGE 2)

1C

**Unclassified**  
Security Classification

## CONTENTS

	page
INTRODUCTION . . . . .	1
Background . . . . .	1
Objective . . . . .	1
Scope . . . . .	3
TEST SPECIMENS . . . . .	3
TEST FLANGES . . . . .	5
TEST ARRANGEMENT . . . . .	7
Pressure Vessels . . . . .	7
Pumps . . . . .	9
Instrumentation . . . . .	9
TEST PROCEDURE . . . . .	11
TEST OBSERVATIONS . . . . .	12
Displacement . . . . .	16
Modes of Failure . . . . .	16
Critical Pressures . . . . .	19
FINDINGS . . . . .	26
CONCLUSIONS . . . . .	27
APPENDIXES	
A - Presentation of Experimental Data . . . . .	28
B - Application of Experimental Data to Design of Pressure-Resistant Windows . . . . .	43
REFERENCES . . . . .	49

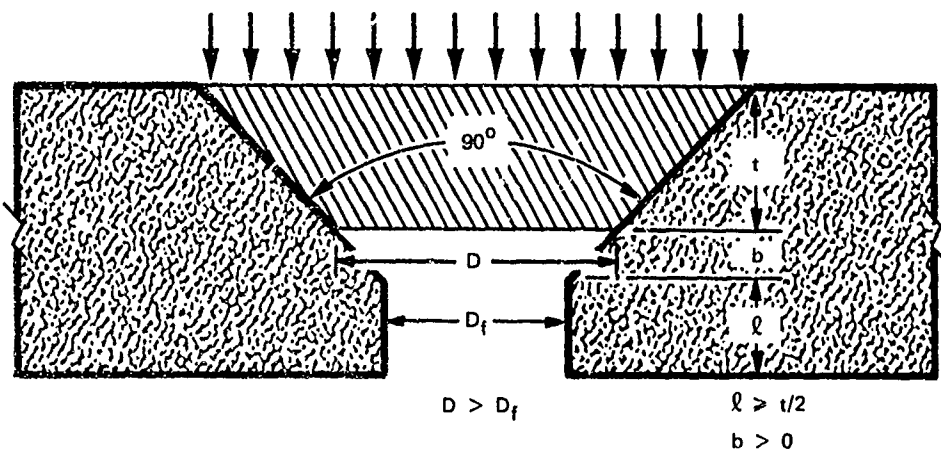
## INTRODUCTION

### Background

Previous studies<sup>1-3</sup> of acrylic windows under short-term hydrostatic pressure were primarily directed towards the effect of hydrostatic pressure on windows of different structural shapes: conical frustums, flat discs, and spherical shell sectors. During the performance of the study of conical frustums,<sup>1</sup> it was discovered that both the ambient temperature and the location of the conical window's low-pressure face with respect to the edge of the beveled bearing surface in the flange cavity have a large effect on the ability of the window to withstand hydrostatic pressure without failure (Figure 1). The critical pressures (pressure at which ultimate failure of window occurs) of conical acrylic windows were found to vary during exploratory tests as much as 30% because of temperature changes in the 32°F-to-90°F range and as much as 60% because of changes in the window's elevation with respect to the bottom edge of the window seat in the flange. Therefore the effect of temperature and window seat elevation could not be considered as negligible. Recognizing the importance of these variables on the design of man-rated windows for undersea habitats, hyperbaric chambers, and internal pressure vessels for ocean simulation facilities, the Naval Facilities Engineering Command sponsored a study in this area as a part of the Ocean Engineering Program of the Naval Civil Engineering Laboratory (NCEL). This report is a summary of that study.

### Objective

The objective of the study was to investigate the effect that (1) the ambient temperature and (2) window location with respect to the edge of the beveled bearing surface in the flange cavity have on the short-term critical pressure of conical acrylic windows. The data resulting from this study will permit the designers of window/flange assemblies for internal or external pressure vessels to (1) predict with greater certainty the ultimate short-term critical pressure of the selected window at any temperature and to (2) optimize the ultimate short-term strength of the window for the desired diameter by selecting the proper relationship between the minor diameter of the window ( $D$ ) and the minor diameter of the conical flange cavity ( $D_f$ ).



Note:  $D$  = minor diameter  
 $D_f$  = minor flange opening diameter  
 $t$  = window thickness

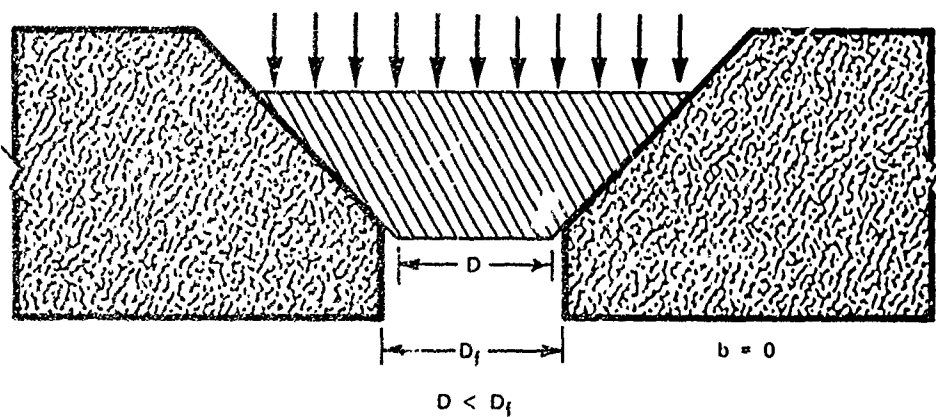
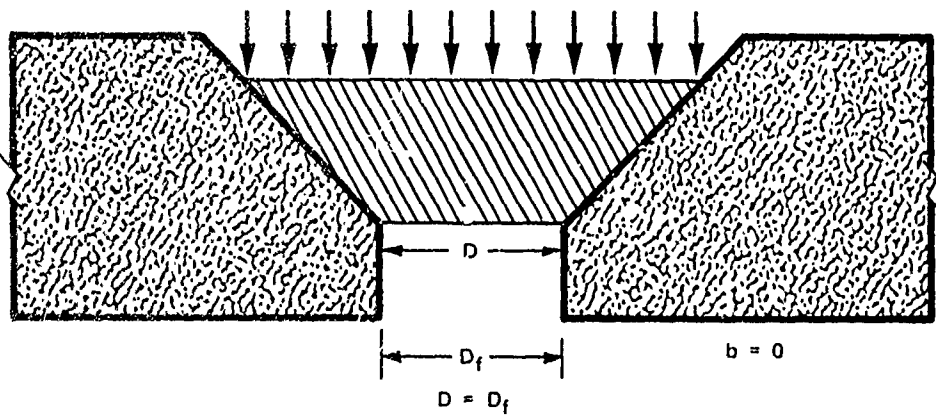


Figure 1. Typical window-seating arrangements for conical frustum acrylic windows. Critical pressure of window is maximized when  $b > 0$ ; magnitude of  $b$  varies with  $t/D$  ratio.

## Scope

The study was conducted experimentally and the relationships between variables derived empirically (Tables 1 and 2). Only short-term pressure loading was utilized to permit completion of the study within the existing framework of funding and pressure vessel availability. Since previous studies<sup>1,4,6</sup> have shown that windows of 90-degree included angle represent a good compromise between critical pressure, extrusion resistance, bulk, and cost for most typical pressure applications, only 90-degree windows were investigated at this time. The temperature variation was limited to 32°F-to-90°F range and it was varied in four discrete steps. The thickness-to-minor-diameter ( $t/D$ ) ratio was varied from 0.083 to 0.775 in six steps; the relationship between minor diameter of the window ( $D$ ) and minor diameter of the conical window cavity in the flange ( $D_f$ ) was varied from 0.970 to 1.500 in seven steps. It was thought that by utilizing four different ambient temperatures, six  $t/D$  ratios, and seven  $D/D_f$  ratios in an experimental study limited to windows with only a single conical angle, an accurate picture would be generated of the interrelationship between these variables for 90-degree windows. Although the data generated by this study are true only for short-term loading conditions, with the proper selection of a safety factor they can serve also as conservative predictors for long-term loading conditions.

## TEST SPECIMENS

The bulk of the test specimens were scale-model 90-degree conical acrylic windows (Figure 2). To validate the experimental data resulting from testing of the model windows, some full-scale windows were to be tested also (Figure 3). Both the model and full-scale windows were machined from commercially available Plexiglas G flat sheets and plates. The machining tolerances for model-scale windows were  $\pm 15$  minutes for the included conical angle,  $\pm 0.002$  inch for the minor diameter, and  $\pm 0.002$  inch for the thickness. Dimensional tolerances for the full-scale windows were  $\pm 15$  minutes for the angle,  $\pm 0.005$  inch for the diameter, and  $\pm 0.010$  inch for the thickness. The machining finish on the models' conical bearing surfaces was 63 rms, while the full-scale windows were polished all over after a finish of 63 rms was imparted by machining. After they were machined and polished, all windows were annealed at 175°F for 24 hours.

Table 1. Test Program for Investigation of Seating Arrangement Effect  
on Critical Pressure of 90-Degree Conical Acrylic Windows

(Material is unshrunk Plexiglas G (Federal Specification  
L-P-391 B); ambient temperature is 68°F to 72°F.)

Minor Diameter, D (in.)	No. of Specimens With Thickness, t of—						
	0.125 in.	0.250 in.	0.375 in.	0.500 in.	0.625 in.	0.750 in.	2,000 in.
0.970	5	5	5	5	5	5	—
1.000	5	5	5	5	5	5	—
1.030	5	5	5	5	5	5	—
1.060	5	5	5	5	5	5	—
1.125	5	5	5	5	5	5	—
1.250	5	5	5	5	5	5	—
1.500	5	5	5	5	5	5	—
3.880	—	—	—	—	—	—	4
4.000	—	—	—	—	—	—	1
4.120	—	—	—	—	—	—	1
4.240	—	—	—	—	—	—	4
4.500	—	—	—	—	—	—	1
5.000	—	—	—	—	—	—	1
6.000	—	—	—	—	—	—	4
6.400	—	—	—	—	—	—	2
8.500	—	—	—	—	—	—	2

Table 2. Test Program for Investigation of Temperature Effect on  
Critical Pressure of 90-Degree Conical Acrylic Windows

(Material is unshrunk Plexiglas G; ambient temperatures are shown below.)

Temperature (°F)	Minor Diameter, D (in.)	No. of Specimens With Thickness, t of—					
		0.125 in.	0.250 in.	0.375 in.	0.500 in.	0.625 in.	0.750 in.
32	1,000	5	5	5	5	5	5
	1,500	5	5	5	5	5	5
50	1,000	5	5	5	5	5	5
	1,500	5	5	5	5	5	5
90	1,000	5	5	5	5	5	5
	1,500	5	5	5	5	5	5

Material: Plexiglas G, Federal Specification L-P-391 B

Nomenclature

D = minor diameter (in.)  
t = thickness (in.)  
 $\alpha$  = included conical angle (deg)

Dimensions

1. Model windows:

D = 0.970, 1.000, 1.030, 1.060, 1.125, 1.250, 1.500 in.;  
tolerance =  $\pm 0.005$   
t = 0.125, 0.250, 0.375, 0.500, 0.625, 0.750 in.;  
tolerance =  $\pm 0.002$   
 $\alpha$  = 90 deg; tolerance =  $\pm 15$  min

2. Full-scale windows:

D = 4.0 in.; tolerance =  $\pm 0.010$   
t = 3.880, 4.000, 4.120, 4.240, 4.500, 5.000, 6.000,  
6.400, 8.500 in.; tolerance =  $\pm 0.010$   
 $\alpha$  = 90 deg; tolerance =  $\pm 15$  min

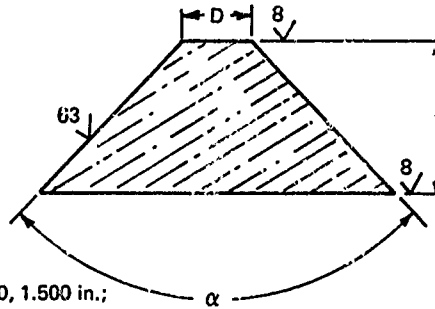


Figure 2. Typical model and full-scale acrylic plastic windows.

Since, from the previous studies<sup>1-12</sup> with acrylic windows and complete acrylic pressure hulls, it is known that the mechanical and physical properties of Plexiglas G do not vary significantly (1) from one sheet of material to another, and (2) between sheets of different thickness, no material test program was undertaken during this study. Because of this reproducibility in material properties inherent in Plexiglas G, it is assumed that all the data generated in this study are interrelated without any conversion factor with the data generated in the previous NCEL window and pressure hull studies that also utilized Plexiglas G material.

## TEST FLANGES

For the testing of windows, two kinds of flanges of 90-degree included angle were employed. The flange for testing models had a window cavity with 1-inch minor diameter (Figure 4a), while the one for the full-scale windows had a 4-inch minor diameter (Figure 4b). In both cases, the dimensional tolerances for the minor diameter were  $\pm 0.001$  inch, while for the included conical angle they were  $\pm 5$  minutes. The machining finish on the conical bearing surface in each case was 63 rms. Since dimensional changes of the flanges can influence the critical pressure of windows significantly, precautions were taken to make the flanges as rigid as possible. Because of the massive construction selected for the flanges, they were assumed to be perfectly rigid with respect to the windows tested.

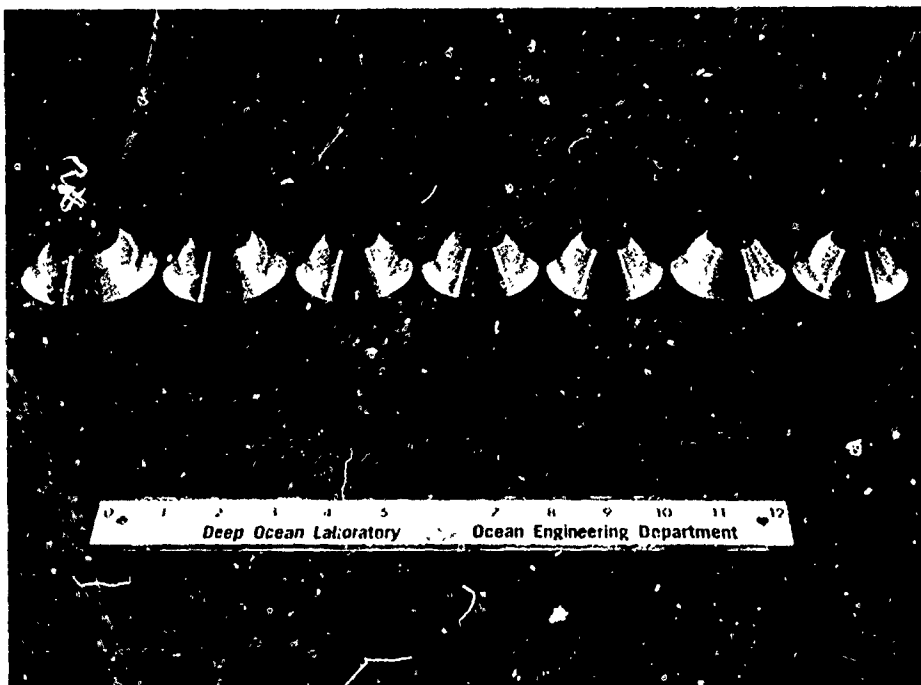


Figure 3a. Typical model acrylic plastic windows.



Figure 3b. Typical full-scale acrylic plastic windows.

Nomenclature

M = external flange diameter (in.)  
 $\alpha$  = included conical angle (deg)

Dimensions

$\alpha$  = 90 deg; tolerance =  $\pm 15$  min  
M = 4 in.

Material: 4130 steel

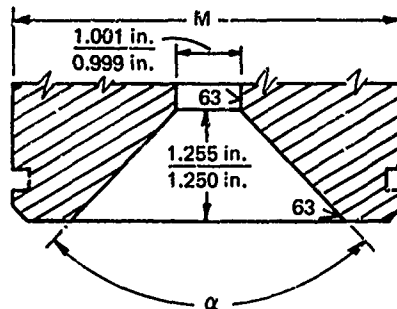


Figure 4a. Dimensions of flange for testing model windows.

Nomenclature

M = external flange diameter (in.)  
L = overall flange thickness (in.)  
k = cylindrical passage length (in.)  
 $\alpha$  = included conical angle (deg)

Dimensions

$\alpha$  = 90 deg; tolerance =  $\pm 5$  min  
M =  $17\frac{3}{4} \pm \frac{1}{64}$  in.  
k =  $1 \pm \frac{1}{64}$  in. for 90-deg windows  
L =  $5 \pm \frac{1}{64}$  in. for 90-deg windows

Material: 4130 steel

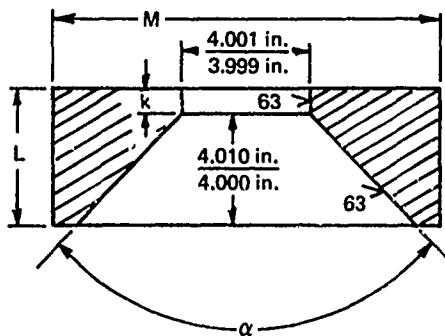


Figure 4b. Dimensions of flange for testing full-scale windows.

## TEST ARRANGEMENT

### Pressure Vessels

The hydrostatic testing of the windows was performed in two different vessels because of the large variation in sizes of windows tested and pressures required for their ultimate failure.

The *model windows* were tested in a 50,000-psi maximum operational pressure vessel. This 50,000-psi operational pressure vessel was a 5-inch-diameter vessel custom-built for testing windows at high pressure (Figure 5). The special features of the vessel are (1) the window flange being integral with the end closure and (2) temperature control in  $32^{\circ}\text{F}$ -to- $120^{\circ}\text{F}$  range.

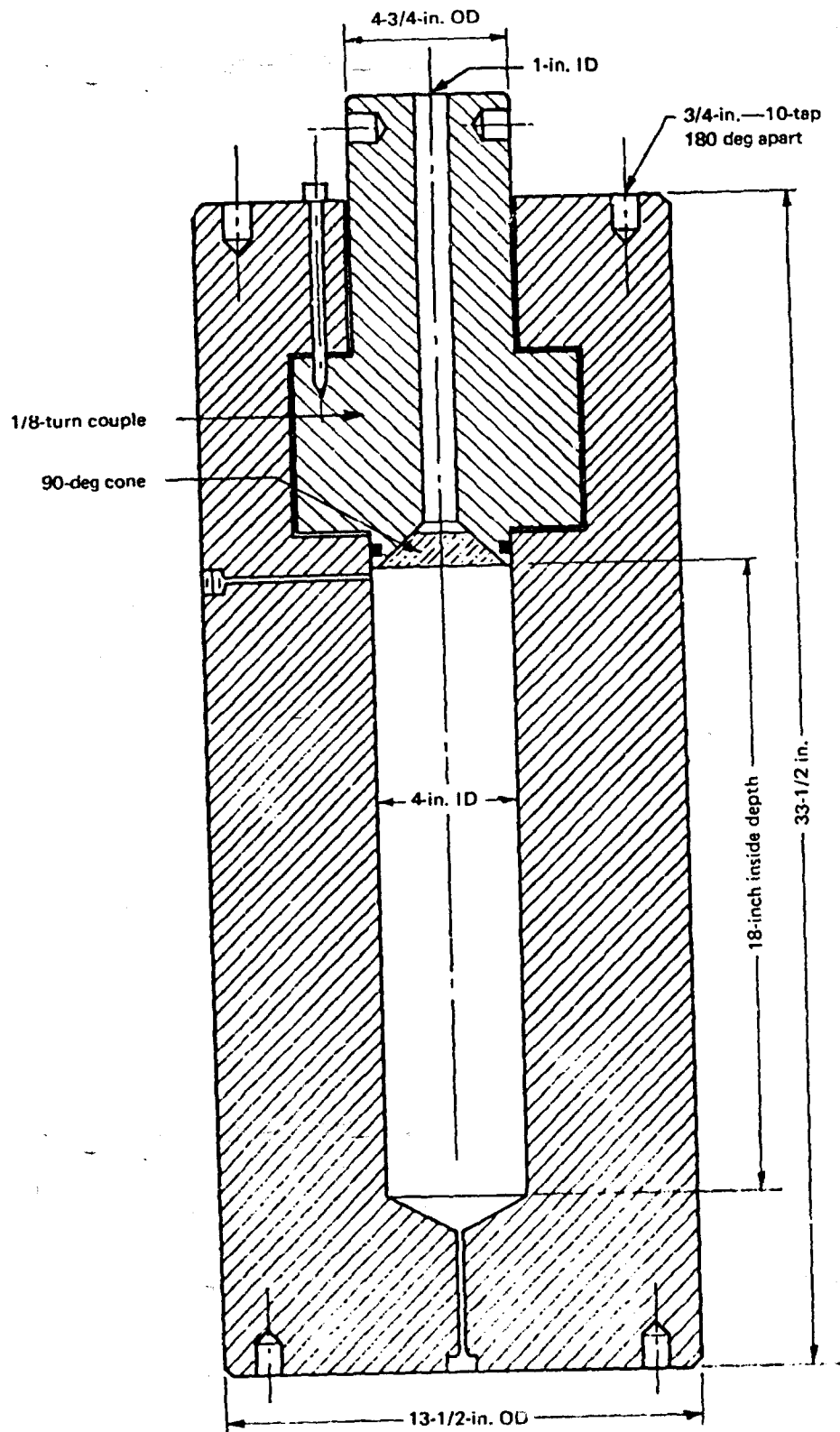


Figure 5. Ocean-pressure simulator with 50,000-psi capability used for testing model windows.

The *full-scale windows* were tested in an 18-inch-diameter vessel with 20,000-psi internal pressure capability (Figure 6). The special features of the vessel were (1) temperature control in 32°F-to-120°F range and (2) trunnion mounting, permitting the orientation of the vessel either in vertical or horizontal attitude.

### Pumps

Pressurization of all the vessels was accomplished by means of air-operated, positive-displacement pumps. The pressurizing medium used in the 18-inch-diameter pressure vessel was tap water, while in the 5-inch-diameter vessel it was hydraulic oil. In all cases, the pressurization rate was controlled by manual throttling of pressurized air operating the pumps. Because of the precision with which the supply of pressurized air could be regulated, the pressurization rate of the vessels could be controlled within ±50 psi/min around the specified 650-psi/min rate.

### Instrumentation

The instrumentation for the measurement of *test conditions* consisted of a remotely reading Bourdon-tube-type thermometer with 1°F resolution and remotely reading Bourdon-tube-type pressure gages with 1-psi resolution in the 0-to-1,000-psi, 10-psi in the 1,000-to-10,000-psi, 20-psi in the 10,000-to-30,000-psi, and 50-psi in the 30,000-to-50,000-psi pressure range. The *displacement* of the window through the flange opening was measured with a mechanical measuring device consisting of a dial indicator, and wire/pulley system connecting the dial indicator with the center of the window's low-pressure face (Figure 7). The wire was anchored to the center of the window's low-pressure face by means of an acrylic post bonded with acrylic cement to the window face. Since the anchor was bonded and not mechanically fastened to the window surface, it did not affect in any manner the window's strength under hydrostatic loading.

The ultimate failure of the window at critical pressure was accompanied by a loud explosion and ejection of a high-pressure jet of water from the vessel's interior through the flange opening. To protect the test personnel from any hazards associated with the forceful emission of water and window fragments, the dial indicator readings were transmitted by television camera and video console system from the vessel to the test control center located behind massive concrete blast deflectors. In this manner, the source of error in the displacement readout system was minimized by keeping the wire between the dial indicator and the window as short as possible while at the same time maximizing the safety of the test operator by removing him from the immediate vicinity of the vessel.

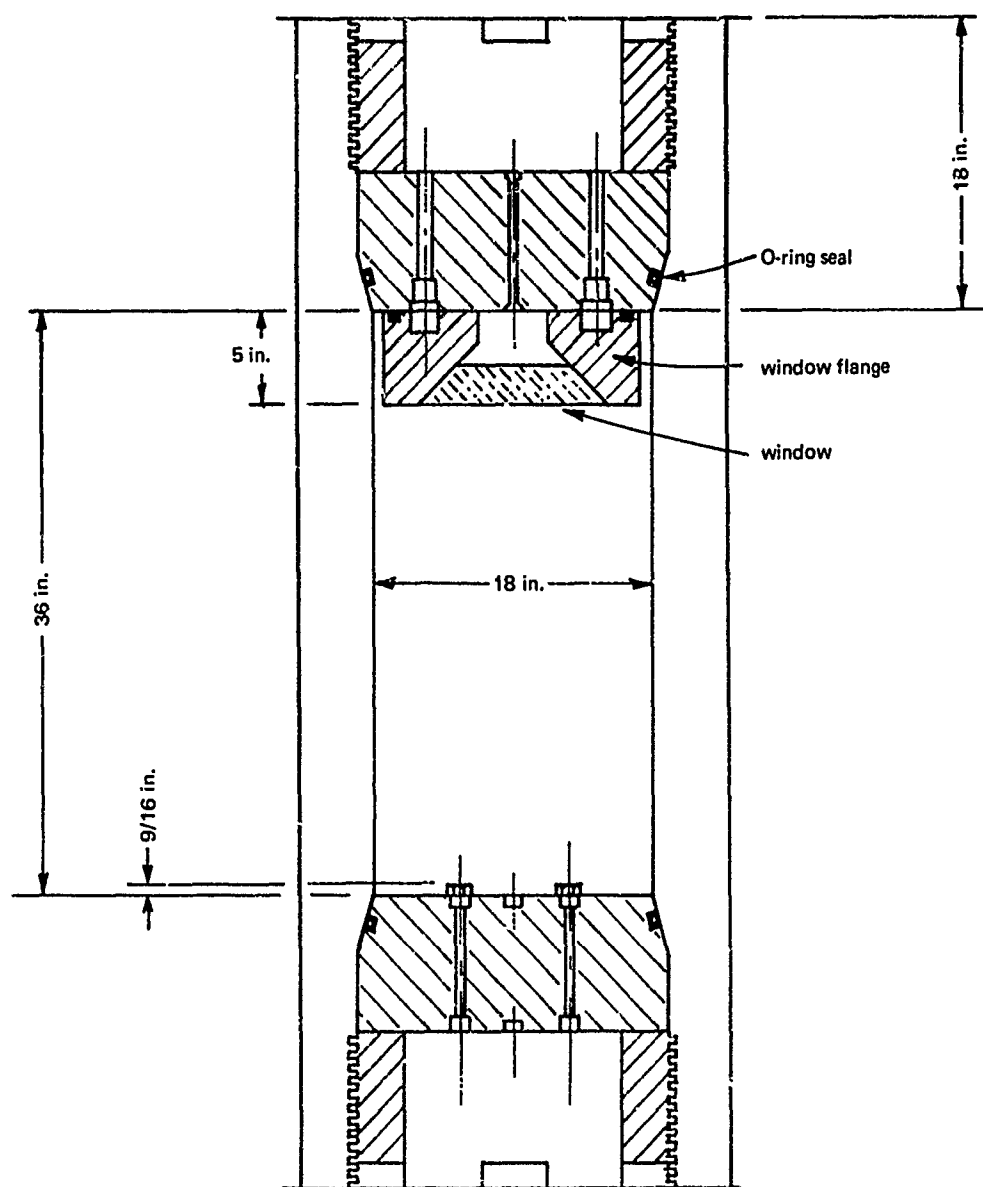


Figure 6. Ocean-pressure simulator with 20,000-psi capability used for testing full-scale windows.

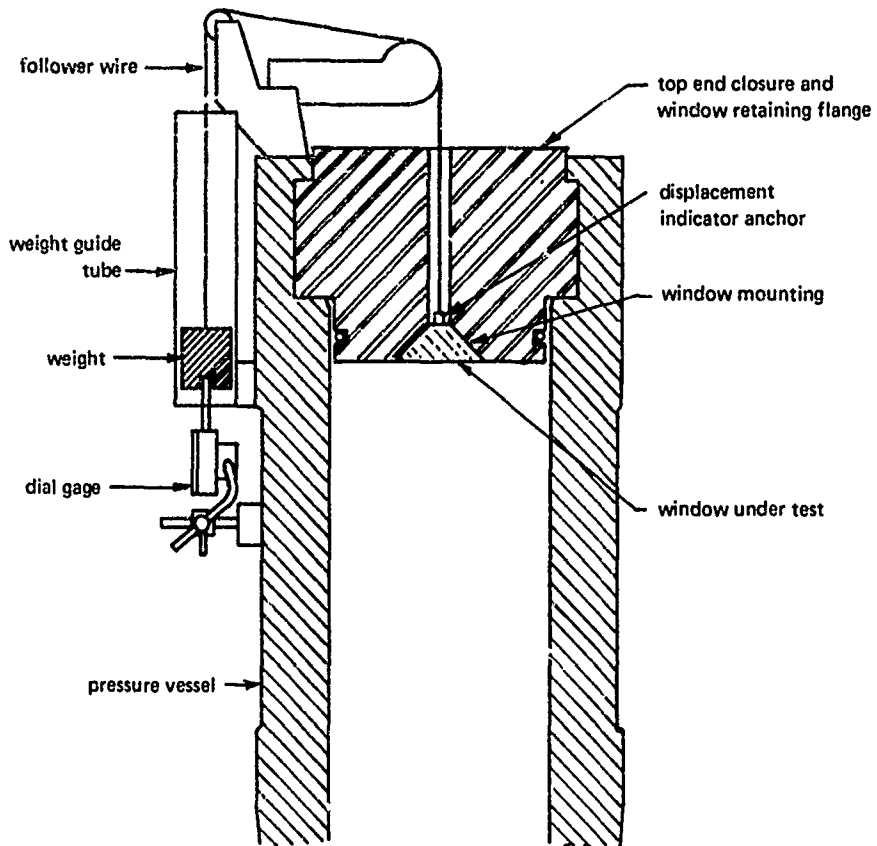


Figure 7. Arrangement for measuring window displacements through retaining flange.

## TEST PROCEDURE

To standardize the test conditions for the window test program, a procedure was developed that was followed during all the tests in this study. This procedure had as its objective to ensure that (1) the thickness of the grease, (2) the length of exposure to ambient water temperature, and (3) the rate of pressurization to failure did not introduce additional variables into the test program.

The effect of grease thickness on the flange seating surface was minimized by preloading each window in the flange with hydrostatic pressure for 5 minutes. The preloading pressure ( $t \times 500$  psi for model windows and  $t \times 125$  psi for full-scale windows) was considered sufficient to squeeze out all the grease surplus from between the window and the flange, while at the same time the pressure was not high enough to induce any permanent deformation of the window. At the conclusion of the preloading period, the pressure on the window was reduced to zero and the displacement measurement system rezeroed by adjusting the dial indicator.

The *effect of temperature exposure duration* was minimized by temperature conditioning all of the windows that were to be tested at temperatures above or below 70°F room temperature. The temperature conditioning was performed by placing the window overnight in a water bath at the same temperature as the pressure vessel before mounting the window into the flange for testing. After removal from the temperature conditioning bath, the window was mounted into the flange (Figures 8 and 9) and immediately lowered (Figures 10 and 11) into the pressure vessel already filled with the pressurizing medium preconditioned to the desired temperature. After locking of the end closure (Figure 12), the windows were immediately hydrostatically preloaded, bringing pressurizing fluid in contact with the window and the end closure. Because the windows were temperature preconditioned and subsequently during the test kept at the desired ambient temperature by leaving the high-pressure face of the window wetted by the pressurizing fluid at preset temperature, it can be safely assumed that the temperature of the acrylic during the application of hydrostatic pressure was essentially the same as the ambient temperature of the pressurizing medium.

The *effect of pressurizing rate* was minimized by controlling the pressurization rate accurately. The pressurization rate was maintained at 650 psi/min with  $\pm 50$ -psi/min variation limits. The selection of 650 psi/min as the standard pressurization rate was based on the fact that all other previous short-term pressurization tests on windows at NCEL utilized this particular rate. In view of this, a comparison of critical pressures for different t/D and D/D<sub>f</sub> ratios or temperatures is feasible, as the pressurization rate in all of these studies was a constant rather than a variable.

## TEST OBSERVATIONS

The test observations were limited to three factors: (1) displacement, (2) mode of failure at critical pressure, and (3) critical pressure. Some aspects of observations (like magnitude of displacement and critical pressure) lent themselves to quantifying and recording in digital form. Other aspects of observations could only be recorded qualitatively. Such aspects were character of displacement (jerky, smooth, sudden, etc.), rate of energy release at failure (loud bang or quiet hiss), and mechanism of failure (flexure, plug extrusion, etc.).

Appendices A and B discuss the presentation of experimental data from the observations and the application of such data to design of pressure-resistant windows.

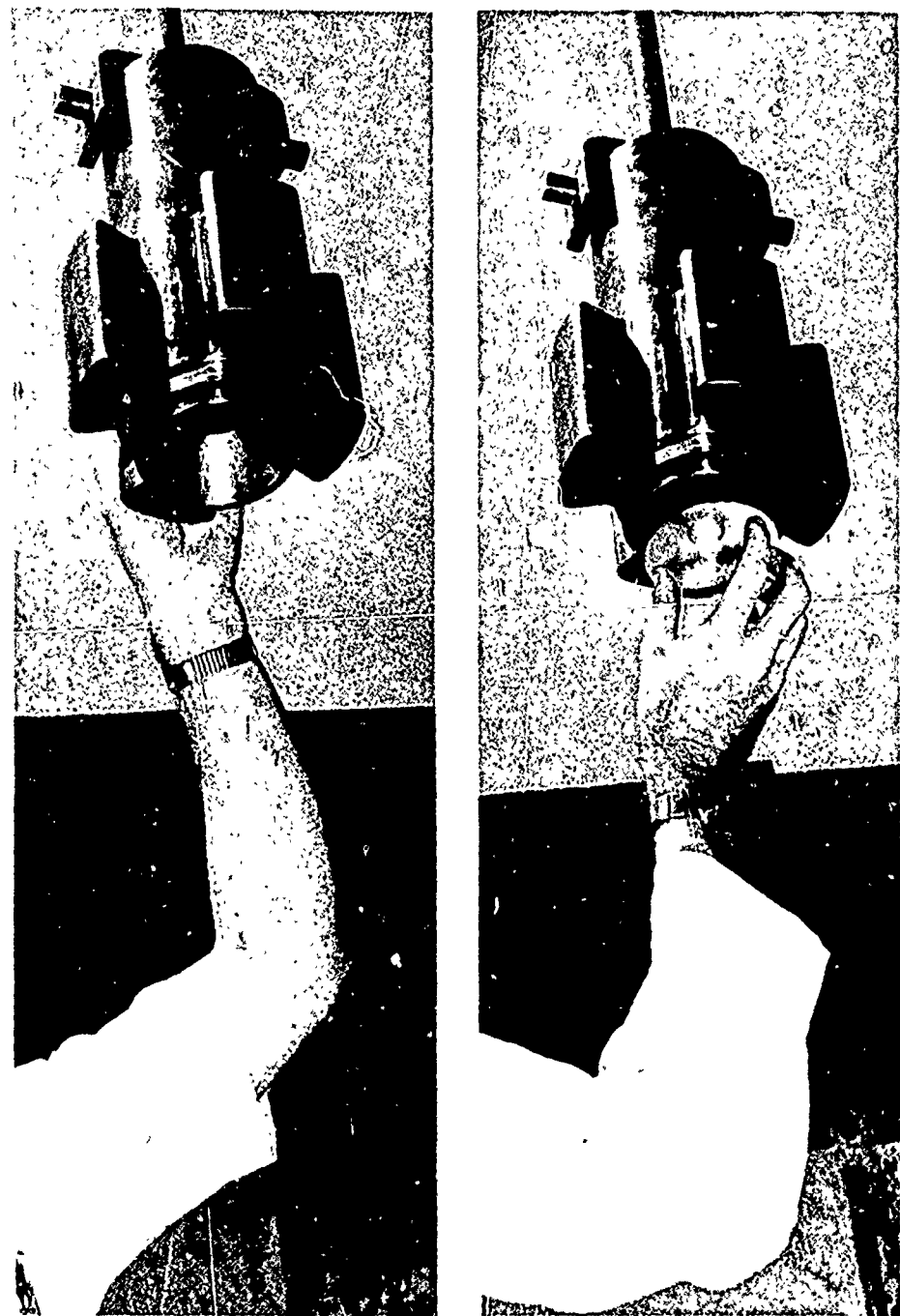


Figure 8. Vessel end closure with integral window flange before installation of model window for testing to 50,000 psi.

Figure 9. Installation of window.

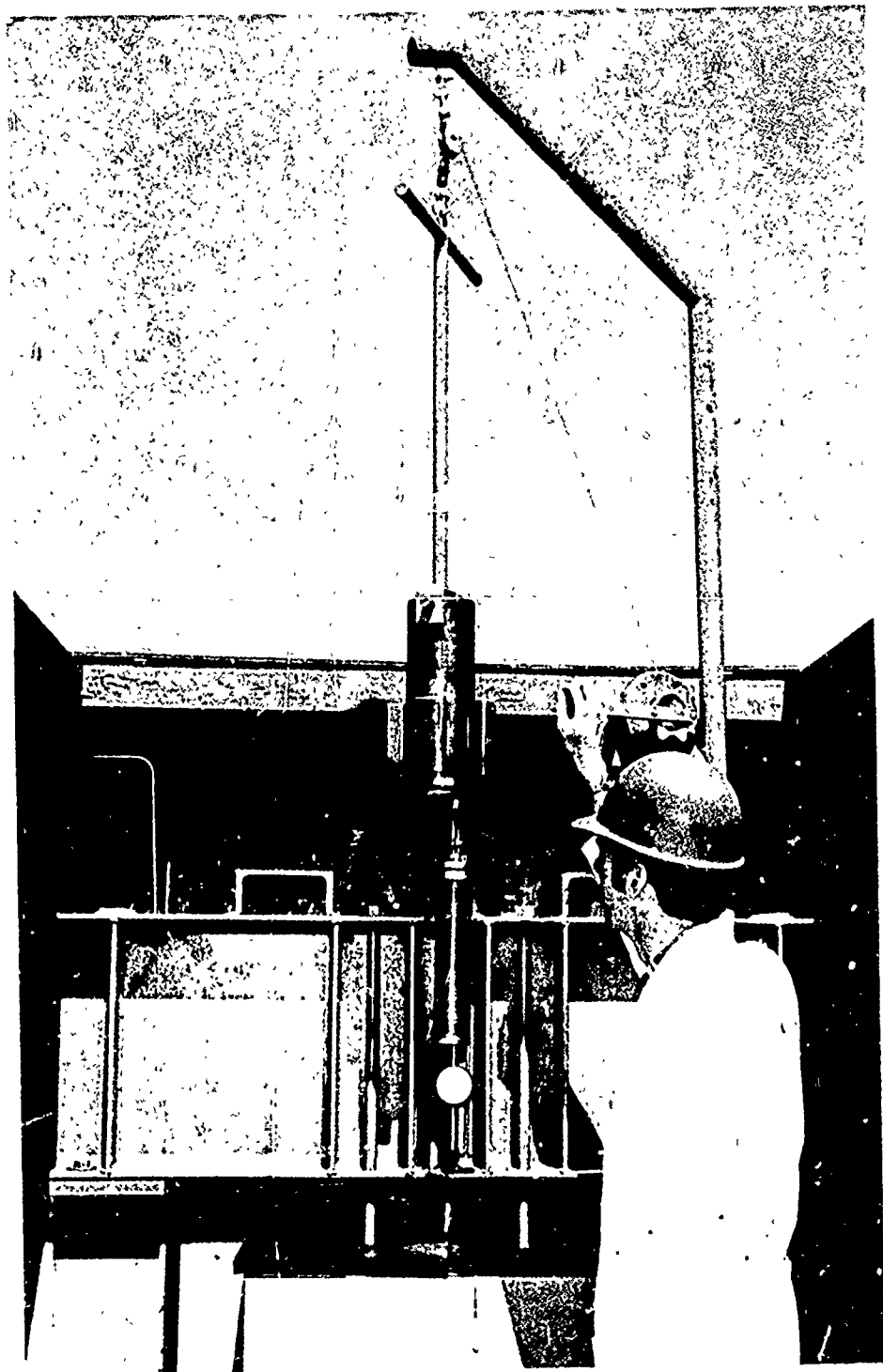


Figure 10. Lowering end closure into pressure vessel.

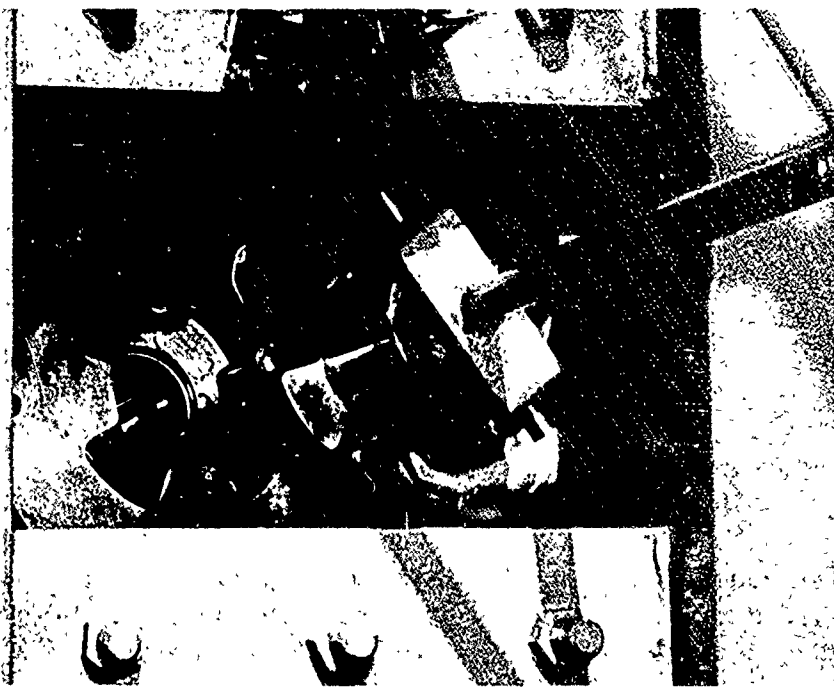


Figure 11. Aligning end closure lugs with slots in pressure vessel.

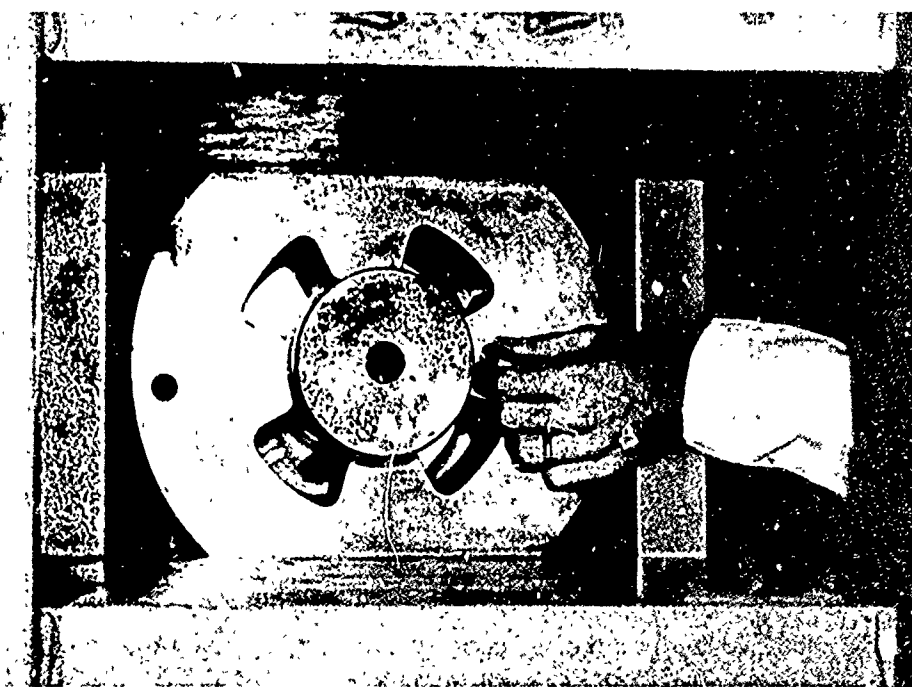


Figure 12. Securing locked assembly with pins.

## Displacement

All windows displaced with an increase in hydrostatic pressure. However, whereas the displacement of windows with  $t/D < 0.125$  was stepped, that of thicker windows was smooth. This stepped displacement coincided with the pulsation in pressure resulting from the action of the positive-large displacement pump on a small volume of contained liquid.

Windows with  $t/D \geq 0.500$  displaced at a reasonably constant rate until moments before failure where an order-of-magnitude increase in displacement rate would take place. Windows with  $t/D \geq 0.625$  did not exhibit a sudden increase in displacement rate at any time before failure. For these windows, the displacement rate was relatively steady and constant until failure actually took place.

The magnitude of displacement was not only a function of the window's  $t/D$  ratio but also of the temperature and the window/flange  $D/D_f$  ratio. For windows of a given  $t/D$  ratio, the magnitude of displacement at any particular pressure was directly related to temperature and inversely to  $D/D_f$  ratio. For example, at  $32^{\circ}\text{F}$  the displacement of windows with  $t/D = 0.500$  under 10,000-psi loading was  $0.22D$  for  $D/D_f = 1.000$ , while for  $D/D_f = 1.500$ , it was  $0.015D$ . At  $90^{\circ}\text{F}$ , the displacement of windows with  $t/D = 0.500$  under 10,000-psi loading was, on the other hand,  $0.051D$  for  $D/D_f = 1.000$  and  $0.032D$  for  $D/D_f = 1.500$  (Appendix A—Figures A-1 through A-13).

## Modes of Failure

Not all of the windows failed, as the pressurizing capability of the pump was limited to 48,000 psi, which in many cases did not prove to be sufficient for blowing out some of the thick windows with  $t/D = 0.750$ . There were basically four modes of failures among those windows that failed, depending on the window's  $t/D$  and window/flange  $D/D_f$  ratios.

The windows with  $t/D = 0.125$ , regardless of their  $D/D_f$  ratio, failed in a pattern typical of thin membranes under flexure: radial cracks radiate from the center of the windows towards the periphery (Figure 13). The destruction of the windows was total, with most of the fragments resembling circular sectors. A sudden loud blast accompanied the failure.

Windows with  $0.250 < t/D < 0.375$ , regardless of their  $D/D_f$  ratio, failed in a pattern typical of thick membranes under flexure: the radial cracks radiate from the center of the windows, but before failure of the window the cracks coalesce into a rough conical fracture surface. The apex of the conical fracture surface intersected the center of the window's high-pressure face, while the base of the fracture surface intersected the

window's low-pressure face at its very edge (in some cases, it intersected the bearing surface near the edge of the low-pressure face). The failure was characterized by (1) very little cold flow on the high- and low-pressure window faces, and by (2) the ejection of the acrylic fragments contained within the fracture cone (Figure 14), and (3) slow release of pressure from the interior of the vessel through the relatively small hole in the window's high-pressure face. The release of pressure was accompanied by a loud hiss rather than a bang.

The windows with  $t/D \geq 0.500$  failed in a manner that was dependent on the window/flange  $D/D_f$  ratio. Windows with  $0.970 \leq D/D_f \leq 1.060$  failed in a manner similar to windows with  $0.250 \leq t/D \leq 0.375$  but with a loud bang. No fragments of the window remained in the flange, since the high-velocity stream of pressurizing fluid ( $P_c > 18,000$  psi) tore from the flange even the annular fragment of the window that was restricting its flow by the relatively small fracture hole in its center.

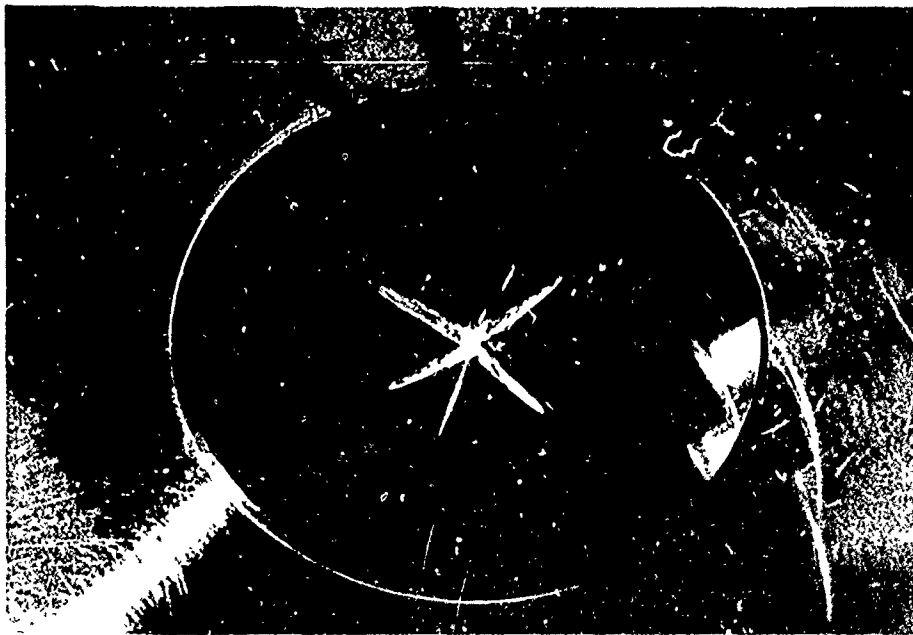


Figure 13. Typical thin-membrane flexure failure of windows with  $t/D \leq 0.125$ ; low-pressure face.

Windows with  $t/D \geq 0.500$ , but window/flange arrangement  $D/D_f \geq 1.125$ , failed in two phases (Figure 15). The *first phase* of the failure was a shear-type failure characterized by (a) large cold-flow cratering on the high-pressure face (Figure 16), (b) considerable cold-flow extrusion on the low-pressure face, and (c) gradual separation of a cone-shaped fragment of acrylic from the rest of the window body. The shear cone intersected



(a) High-pressure face.



(b) Low-pressure face.

Figure 4. Typical thick-membrane flexure failure of windows with  $0.250 \leq t/D \leq 0.375$ .

both the high-pressure face and the bearing area of the window. Interestingly enough, the bearing surface was intersected approximately midway between the low- and high-pressure faces. The intersection of the shear cone and of the high-pressure face resulted in a penetration significantly larger than the penetrations observed during failure of windows with  $t/D$  ratio in the 0.250-to-0.375 range. Measurement of the penetration diameter revealed that it was invariably equal to or slightly larger than the  $D_f$  of the flange, while the penetrations for the  $0.250 \leq t/D \leq 0.375$  windows were generally less than  $0.5D_f$  of the flange.

Another interesting feature of the shear-cone failure was the smoothness of the conical fracture (Figure 16) surface, so strikingly different from the roughness of the flexure-type fracture surface found in 0.250 and 0.375  $t/D$  windows. No flow of water took place during the first phase of the failure, as the central fragment of the window was still substantial enough to act as a plug in the flange.

The *second phase* of the failure was a massive flow extrusion failure of the central window fragment. During this phase while the central window fragment was extruded through the minor flange diameter, the annular window fragment resulting from the shear failure of the first phase did not see any further action, as it was subjected now only to purely isostatic loading. The second phase of failure concluded after further operation of the pressurizing pump with the forceful ejection of the central window fragment through the small bottom opening in the flange cavity. Since the diameter of the penetration in the annular window fragment was larger than the diameter of the small bottom opening in the flange, no restriction was imposed on the jet of rapidly escaping pressurizing medium and thus the annular window fragment was not torn from the flange during the rapid depressurization.

### Critical Pressures

The magnitude of critical pressures was found to be a function of temperature, and  $D/D_f$ , and  $t/D$  ratios. The fact that the critical pressure of a window is a function of these variables was established in previous studies, but only the effect of  $t/D$  ratio was quantitatively described. This study permitted quantitative establishment of the effect of  $D/D_f$  and temperature also. Comparison was made of the magnitudes of critical pressures for windows with different  $t/D$  and  $D/D_f$  ratios but at the same ambient temperature. It was noted that the  $D/D_f$  ratio has a very significant effect on the critical pressure of some windows but a negligible effect on others, depending on their  $t/D$  ratio (Figure 17). In general, as the  $t/D$  ratio increased so did the effect of the  $D/D_f$  ratio. For  $t/D$  ratios  $\leq 0.300$ , the

effect of changing the  $D/D_f$  ratio for a given  $t/D$  ratio was negligible, while for  $t/D$  ratios  $\geq 0.300$ , the effect was significant. For example, windows with  $t/D = 0.500$  experienced a gain in critical pressure of approximately 20,000 psi (about 100%) when the  $D/D_f$  parameter was varied from 0.970 to 1.500. For windows with larger  $t/D$  ratios, the effect should be even more pronounced, but the lack of experimental data on windows with  $t/D > 0.500$  precludes any quantitative description (Appendix A—Figures A-14 through A-19).

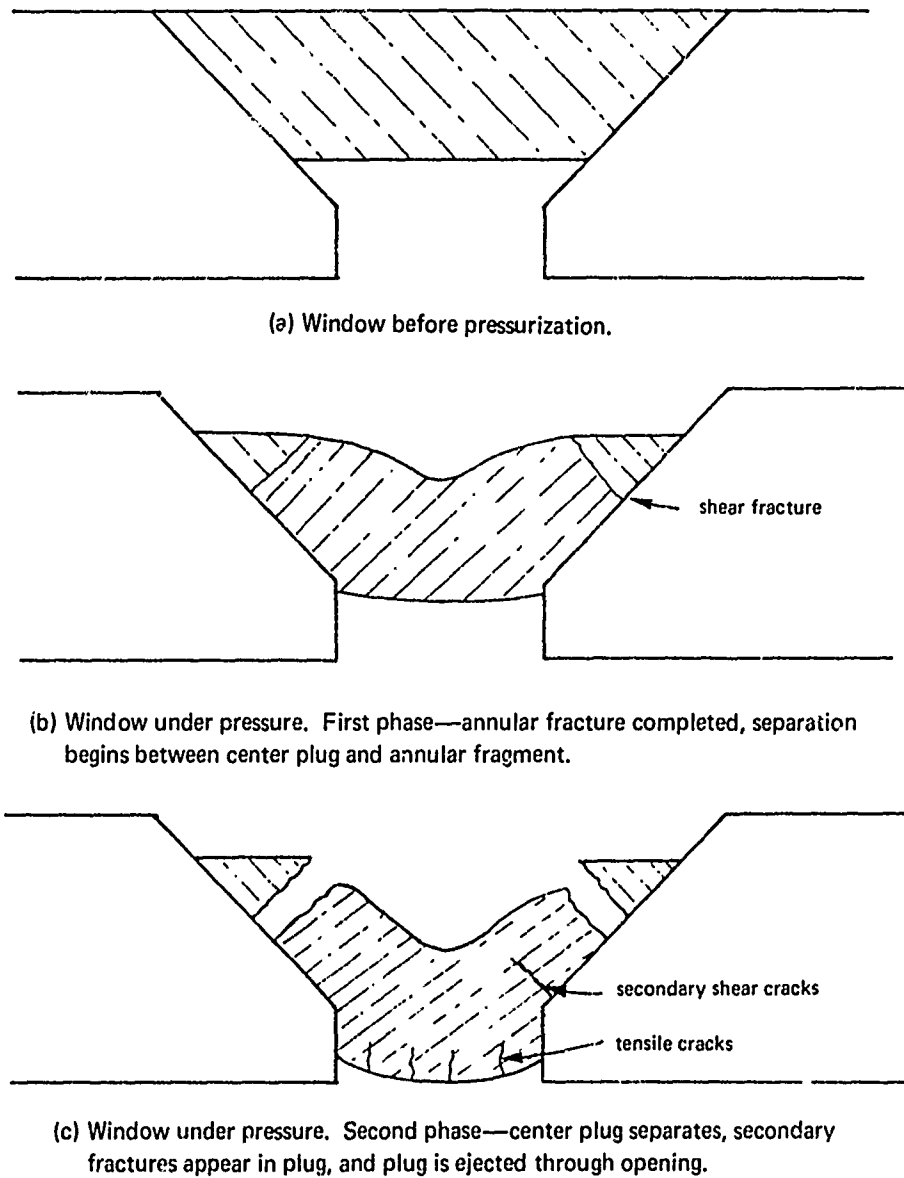


Figure 15. Shear failure mechanism in windows with  $t/D \geq 0.500$ .



(a) High-pressure face of fractured window.



(b) High-pressure faces of fragments after disassembly of fractured window.



(c) Low-pressure face of fractured window.



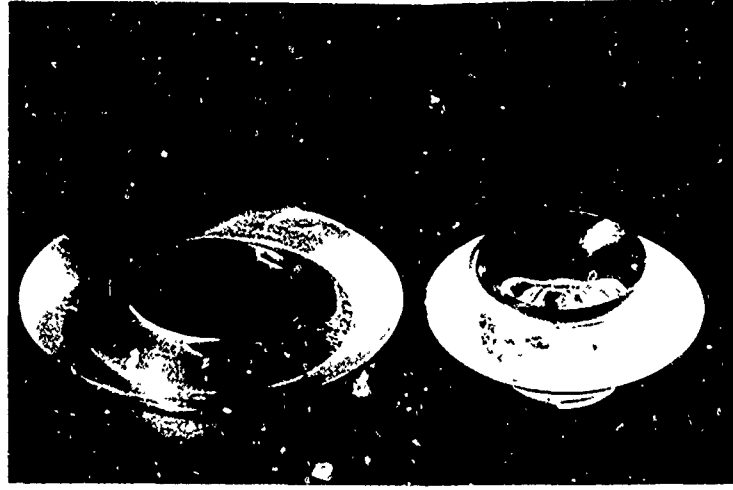
(d) Low-pressure faces of fragments after disassembly of fractured window.

Reproduced from  
best available copy.

Figure 16. Typical shear failure in windows with  $t/D \geq 0.500$  and  $D/D_f = 1.500$ .



(a) High-pressure face of fractured window.



(b) High-pressure faces of fragments after disassembly of fractured window.



(c) Low-pressure face of fractured window.



(d) Low-pressure faces of fragments after disassembly of fractured window.

Reproduced from  
best available copy.

Figure 16. Typical shear failure in windows with  $t/D \geq 0.500$  and  $D/D_f = 1.500$ .

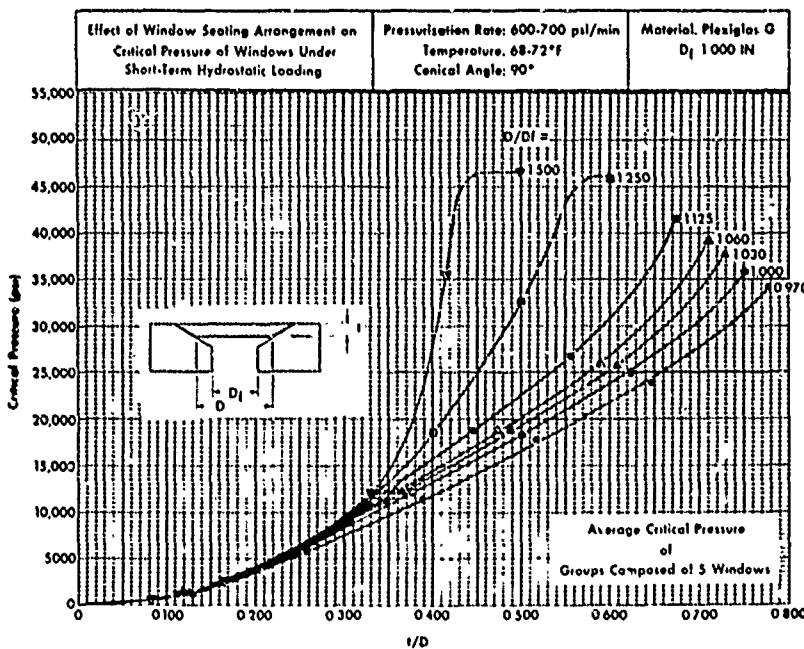
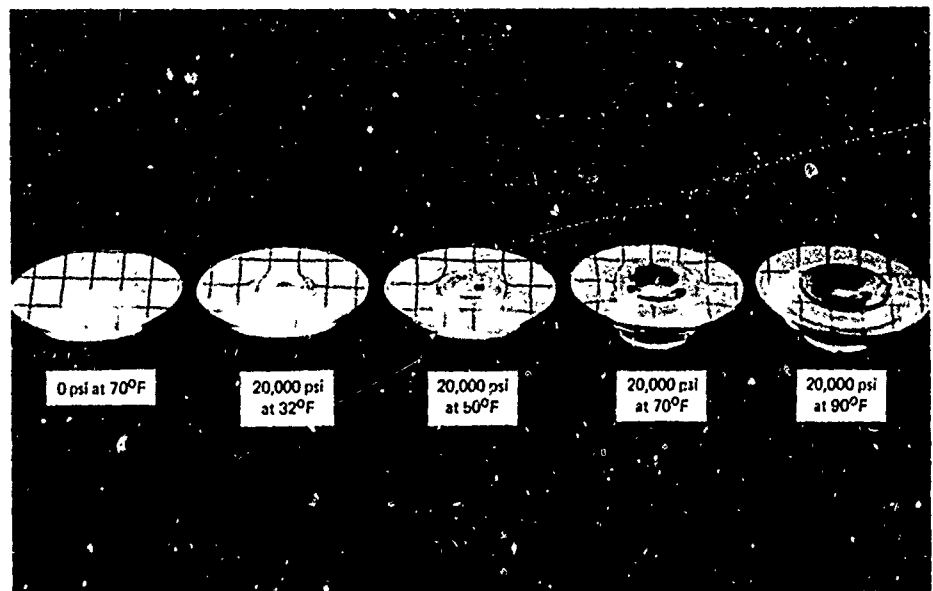


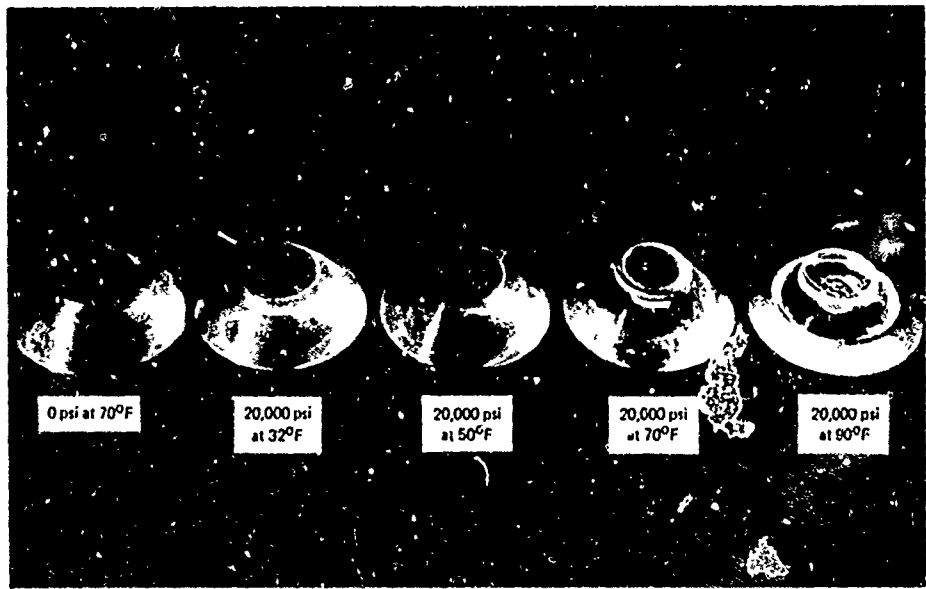
Figure 17 Effect of seating arrangement and  $t/D$  ratio on critical pressure of conical acrylic windows under short-term hydrostatic loading in 68°F-to-72°F temperature range.

Ambient temperature was noted to have a significant effect (Figure 18) on the critical pressure also, but its effect in the 32°F-to-90°F range was as a rule considerably less than that of the  $D/D_f$  ratio (Figure 19). It appears that the temperature changed the critical pressures by the same percentage regardless of their  $t/D$  or  $D/D_f$  ratio. To use again the 0.500  $t/D$  windows as an example, the gain in critical pressure when the temperature was decreased from 90°F to 32°F was approximately 7,300 psi (about 45%).

The scatter in critical pressures for each group (expressed in percent of group's mean) of windows composed of five identical test specimens varied with the  $t/D$  ratio (Figures A-14 through A-19). For groups with  $t/D \leq 0.250$  the total scatter was in the 40-to-30% (of calculated group's mean) range, while for windows with  $t/D > 0.375$  it was in the 3-to-10% range. It would thus appear that the predominant reasons for magnitude-of-scatter range are variations in surface finish and bevel-angle mismatch which vary at random and which cause a discrete difference in critical pressure between individual window specimens regardless of the window's thickness. Since the critical pressures of thin windows are low, the small, discrete differences in critical pressure are interpreted as a larger percentage in scatter than for thick windows, which have high critical pressures. No change in scatter magnitude was observed to be associated with changes in ambient temperature, which substantiated the observations of other studies that the notch sensitivity of acrylic plastic does not increase with a decrease in temperature.<sup>13</sup>

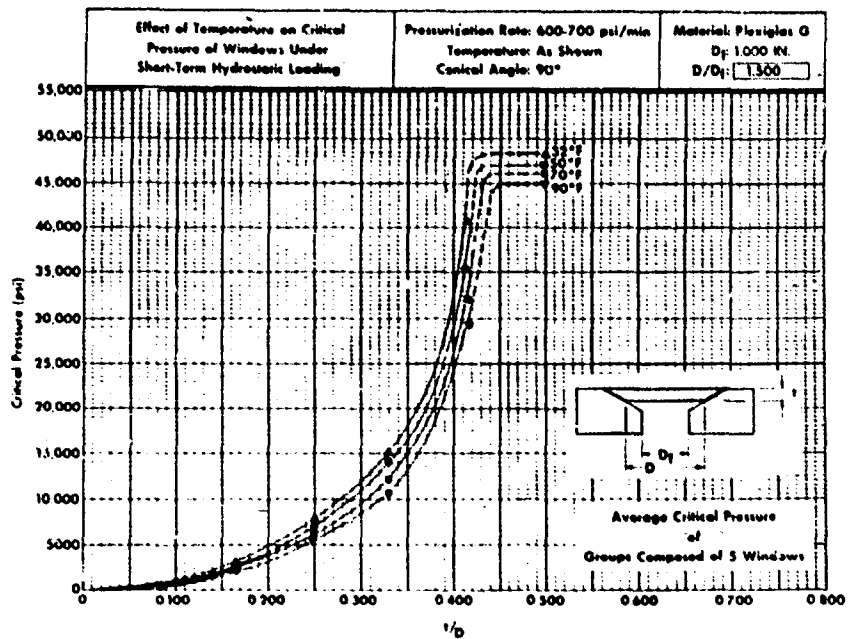


(a) High-pressure faces.

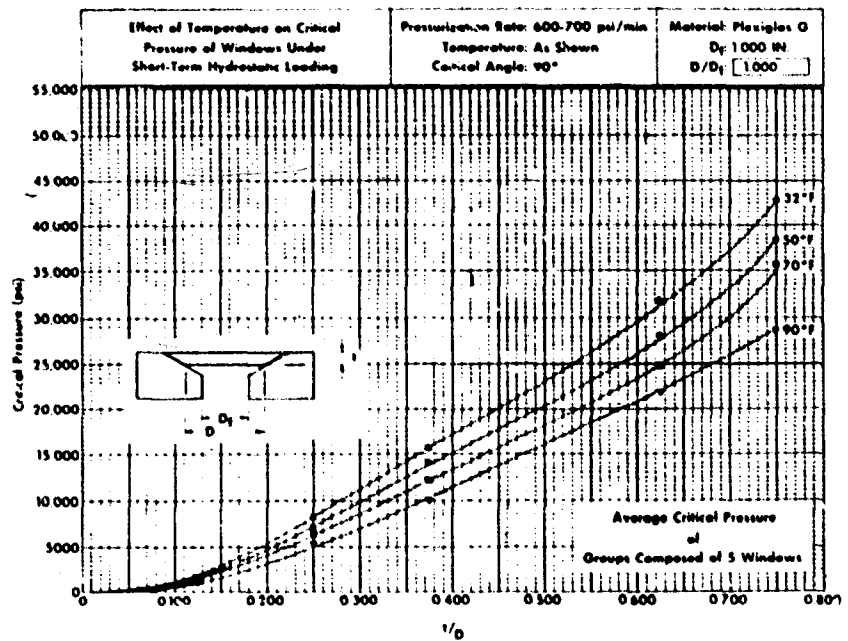


(b) Low-pressure faces.

Figure 18. Effect of ambient temperature on permanent deformation of 90-degree conical acrylic windows subjected to sustained 20,000-psi hydrostatic loading for 1 hour;  $t/D = 0.625$ ,  $D/D_f = 1.000$ .



(a)  $D/D_f = 1.500$ .



(b)  $D/D_f = 1.000$ .

Figure 19. Effect of ambient temperature and  $t/D$  ratio on critical pressure of 90-degree conical acrylic windows under short-term hydrostatic loading.

No difference was observed between the magnitudes of critical pressures for model (Figure A-17), and full-scale windows (Figure A-20), with the same  $t/D$  and  $D/D_f$  ratios under identical ambient temperatures. This (1) further substantiates findings of previous studies denoting that  $t/D$  is a valid nondimensional factor, and (2) establishes the fact the  $D/D_f$  is also a valid nondimensional factor useful in design of window/flange systems.

## FINDINGS

All findings are based on conical acrylic plastic windows of 90-degree included angle and thus apply *quantitatively* to such windows only. These findings also apply to conical windows with other included angles, but only in a qualitative manner.

1. The mismatch ( $D/D_f$  ratio) between minor diameter of the window ( $D$ ) and minor diameter of the conical window cavity in the flange ( $D_f$ ) affected significantly the critical pressure ( $P_c$ ) of acrylic conical windows. The magnitude of increase in  $P_c$  was directly related to the window's  $t/D$  and  $D/D_f$  ratios, but it became significant only for windows with  $t/D \geq 0.300$  and  $D/D_f > 1.030$ . The magnitude of the increase in  $P_c$  (above  $P_c$  associated with  $D/D_f = 1.0$ ) due to  $D/D_f$  ratios  $\geq 1.500$  exceeded 100% for windows with  $t/D \geq 0.500$ .
2. The change in ambient temperature also affected significantly the critical pressure of conical acrylic windows. The relative (in terms of percent) increase in  $P_c$  was independent of  $t/D$  and  $D/D_f$  ratios, but it was inversely related to the ambient temperature of the pressurizing medium. The increase in  $P_c$  was of 30%-to-50% magnitude in the  $32^{\circ}\text{F}$ -to- $90^{\circ}\text{F}$  ambient temperature range.
3. The scatter of  $P_c$  values for identical windows tested under the same test conditions was independent of ambient temperature and was in the 30%-to-40% range for windows with  $t/D \leq 0.250$  ratios and 3%-to-10% range for  $t/D \geq 0.375$  ratios.
4. The  $D/D_f$  ratio, a quantitative indicator of window location in the conical cavity of the flange, was found to be a truly nondimensional parameter like the  $t/D$  ratio.

## CONCLUSIONS

Designers of conical acrylic plastic windows should pay as much attention to the selection of the proper window-seating ratio ( $D/D_f$ ) as to the choice of thickness-to-diameter ratio ( $t/D$ ), because with judicious selection of  $D/D_f$  ratio they can double the critical pressure of such windows.

## Appendix A

### PRESENTATION OF EXPERIMENTAL DATA

#### DISPLACEMENTS

The displacements of windows have been presented as the averages of each window group with the same  $t/D$ ,  $t/D_f$ , and  $D/D_f$  ratios tested under the same ambient temperature. Since there were generally about five windows in each group, the plotted averages represent fairly reliable typical displacement values for windows with a given set of dimensional parameters. The displacements of model windows tested in flanges with  $D_f = 1.000$  inch have been plotted separately (Figures A-1 through A-13) from the displacements of full-scale windows (Figures A-21 through A-28) so that a comparison could be made between the displacements of model and full-scale windows with identical dimensional parameters. The comparison indicates that the displacements of full-scale windows are larger than those of model windows by a scaling factor that can be represented as the ratio of full-scale to model window diameters. In some cases the displacements were smaller for the full-scale windows than predicted by the scaling factor, but in no cases were they any larger.

#### CRITICAL PRESSURES

The critical pressures of window groups have been plotted in such a manner that not only the average but also the maximum and minimum values are shown (Figures A-14 through A-20). This method of plotting was selected to give the window designers an appreciation for typical ranges of critical pressures associated with given  $t/D_f$  and  $D/D_f$  ratios. Comparison of critical pressures for model (Figure A-17) and full-scale windows (Figure A-20) indicated that they are the same if the dimensional and test parameters of windows are the same. The typical range of critical pressures for the full-scale windows (Figure A-20) was found to be also of the same magnitude as for the model windows (Figure A-17), indicating that the critical pressure data generated by testing of model windows are applicable without any scaling or conversion factors to full-scale windows.

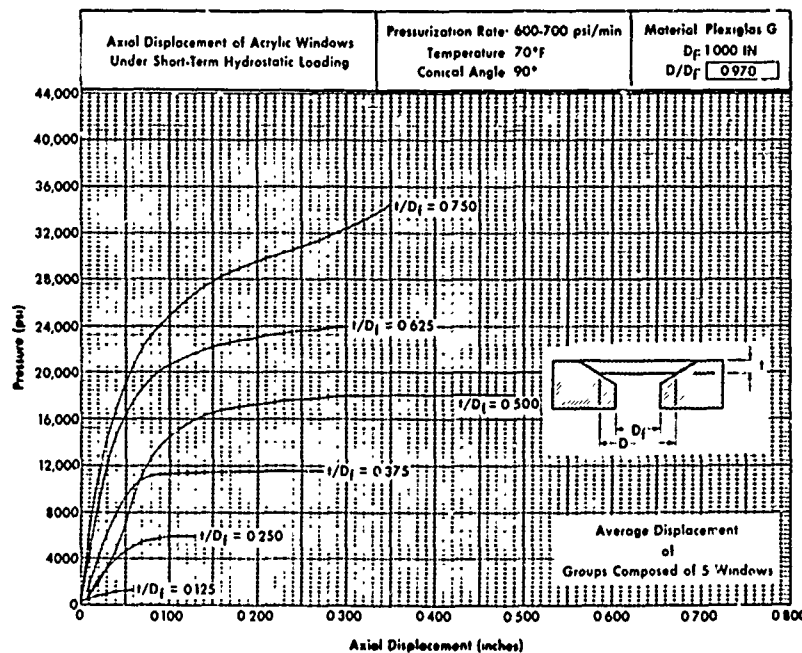


Figure A-1. Effect of short-term hydrostatic loading on axial displacement of 90-degree conical acrylic windows at 70°F ambient temperature;  $D_f = 1.000$  inch,  $D/D_f = 0.970$ .

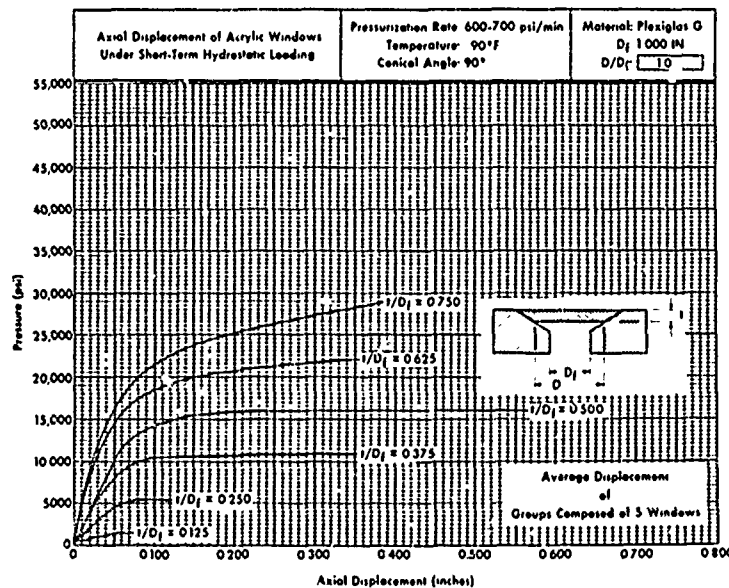
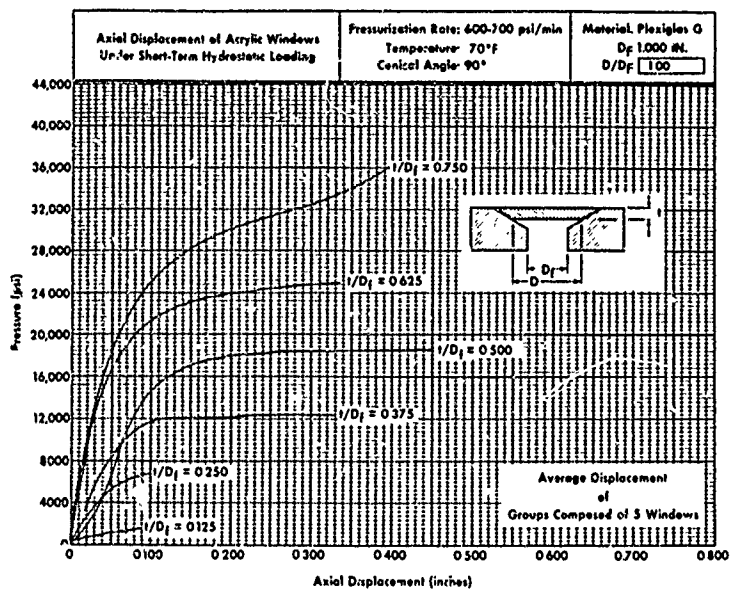
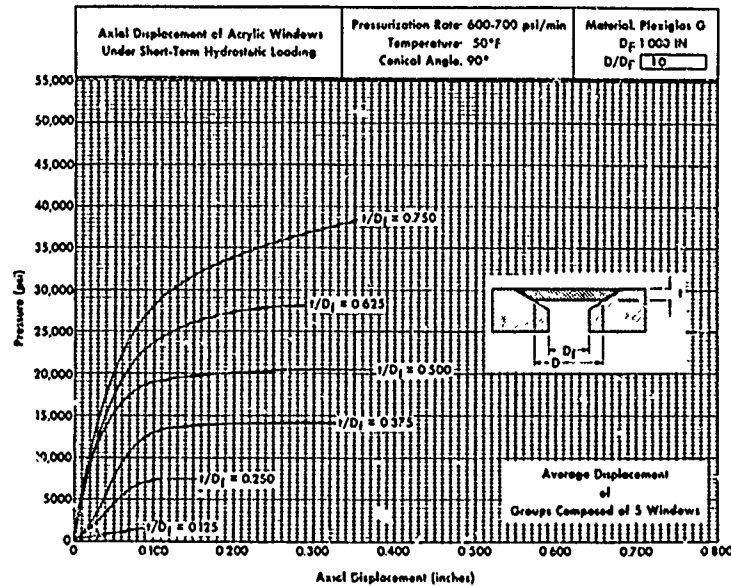


Figure A-2. Effect of short-term hydrostatic loading on axial displacement of 90-degree conical acrylic windows at 90°F ambient temperature;  $D_f = 1.000$  inch,  $D/D_f = 1.000$ .



**Figure A-3.** Effect of short-term hydrostatic loading on axial displacement of 90-degree conical acrylic windows at 70°F ambient temperature;  $D_f = 1.000$  inch,  $D/D_f = 1.000$ .



**Figure A-4.** Effect of short-term hydrostatic loading on axial displacement of 90-degree conical acrylic windows at 50°F ambient temperature;  $D_f = 1.000$  inch,  $D/D_f = 1.000$ .

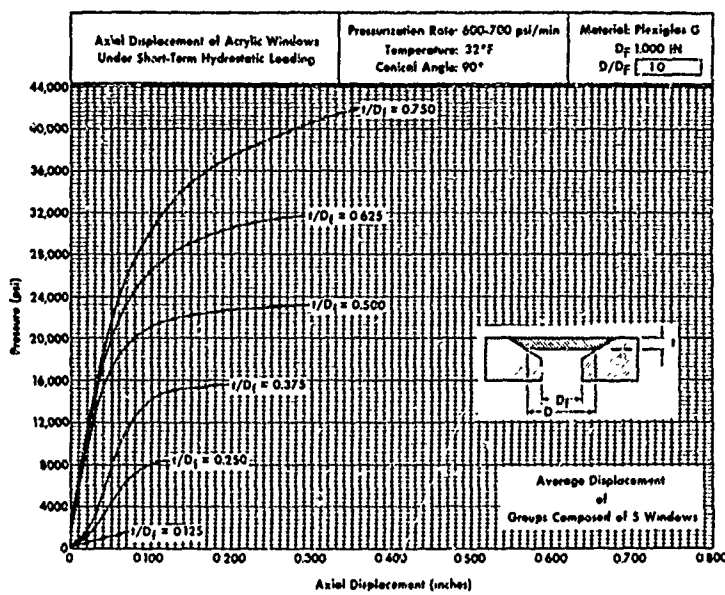


Figure A-5. Effect of short-term hydrostatic loading on axial displacement of 90-degree conical acrylic windows at 32°F ambient temperature;  $D_f = 1.000$  inch,  $D/D_f = 1.000$ .

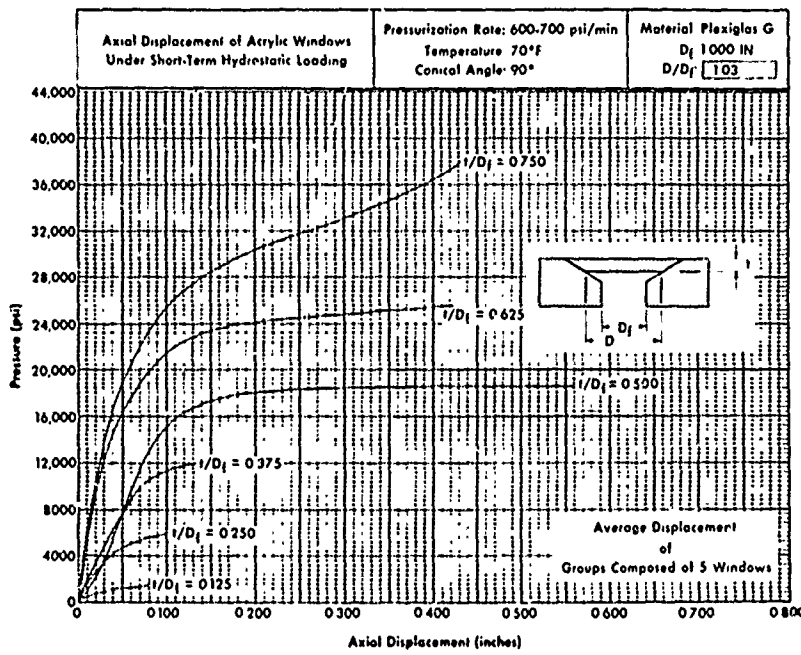


Figure A-6. Effect of short-term hydrostatic loading on axial displacement of 90-degree conical acrylic windows at 70°F ambient temperature;  $D_f = 1.000$  inch,  $D/D_f = 1.030$ .

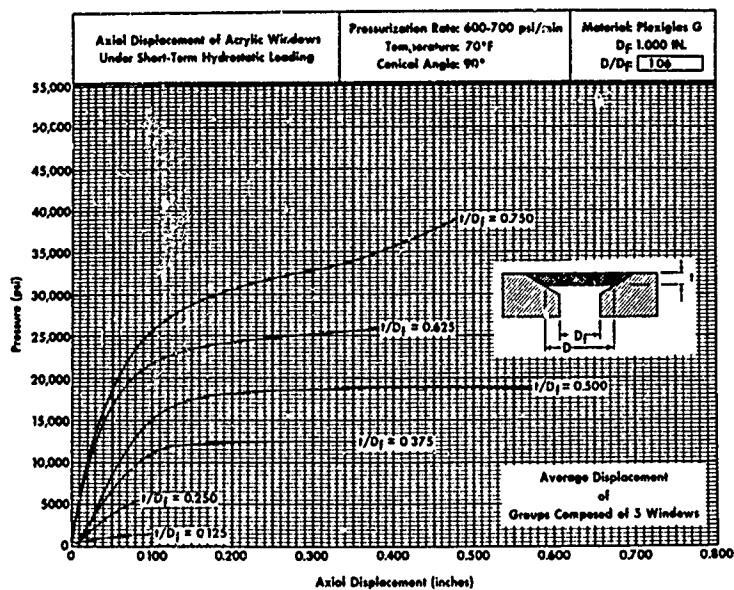


Figure A-7. Effect of short-term hydrostatic loading on axial displacement of 90-degree conical acrylic windows at 70°F ambient temperature;  $D_f = 1.000$  inch,  $D/D_f = 1.060$ .

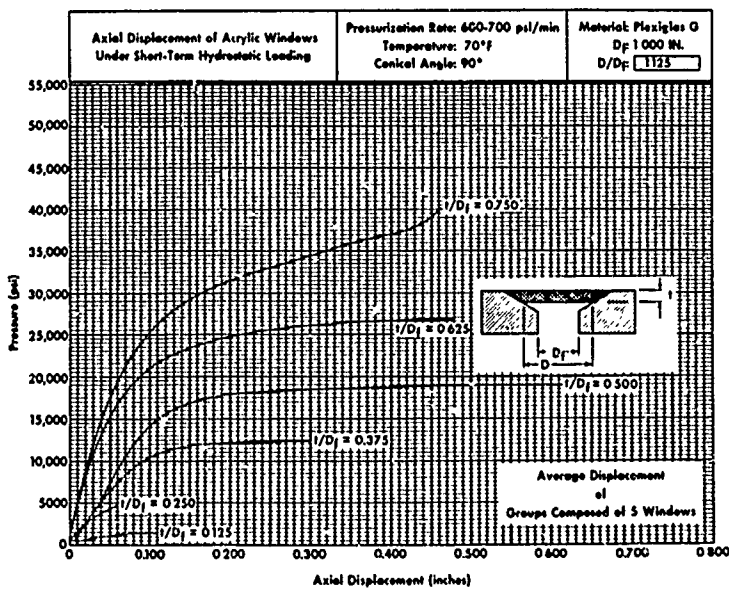


Figure A-8. Effect of short-term hydrostatic loading on axial displacement of 90-degree conical acrylic windows at 70°F ambient temperature;  $D_f = 1.000$  inch,  $D/D_f = 1.125$ .

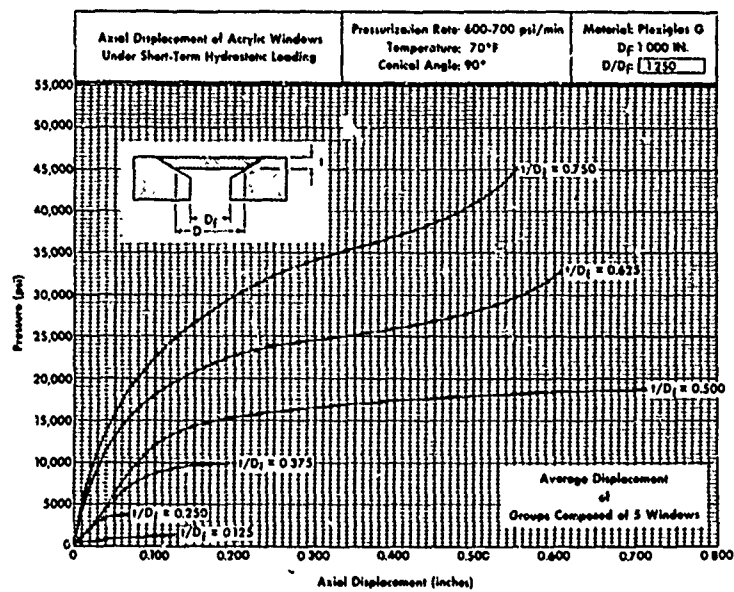


Figure A-9. Effect of short-term hydrostatic loading on axial displacement of 90-degree conical acrylic windows at 70°F ambient temperature;  
 $D_f = 1.000$  inch,  $D/D_f = 1.250$ .

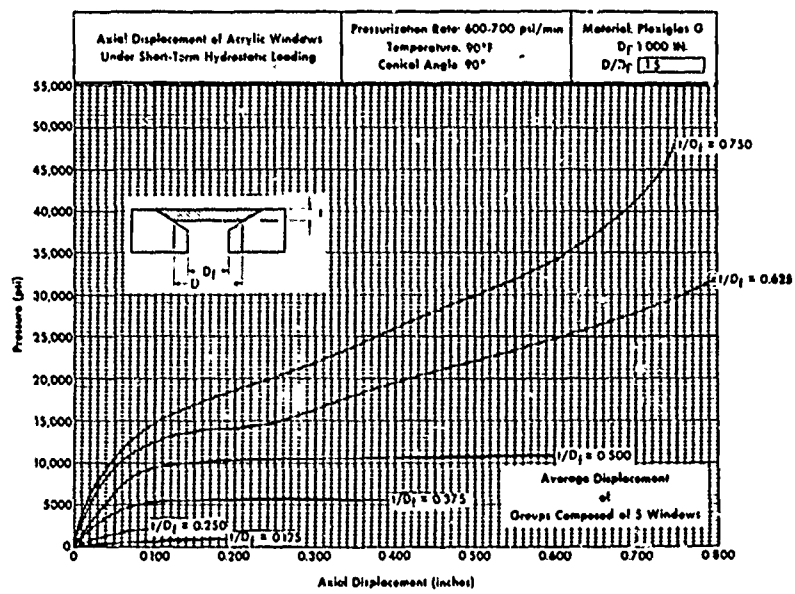


Figure A-10. Effect of short-term hydrostatic loading on axial displacement of 90-degree conical acrylic windows at 90°F ambient temperature;  
 $D_f = 1.000$  inch,  $D/D_f = 1.500$ .

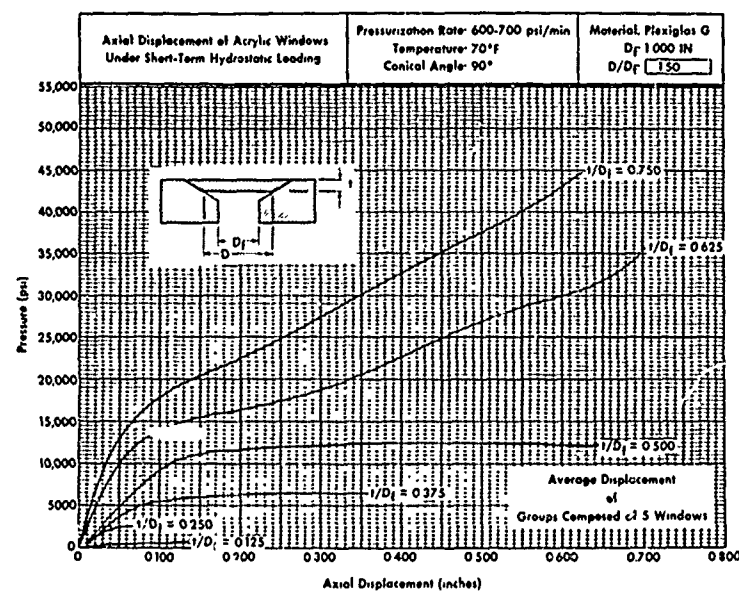


Figure A-11. Effect of short-term hydrostatic loading on axial displacement of 90-degree conical acrylic windows at 70°F ambient temperature;  $D_f = 1.000 \text{ inch}$ ,  $D/D_f = 1.500$ .

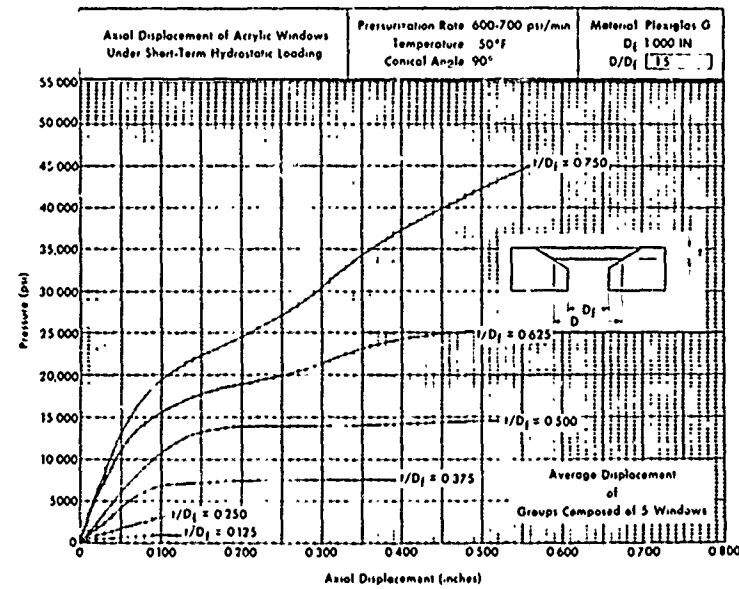


Figure A-12. Effect of short-term hydrostatic loading on axial displacement of 90-degree conical acrylic windows at 50°F ambient temperature;  $D_f = 1.000 \text{ inch}$ ,  $D/D_f = 1.500$ .

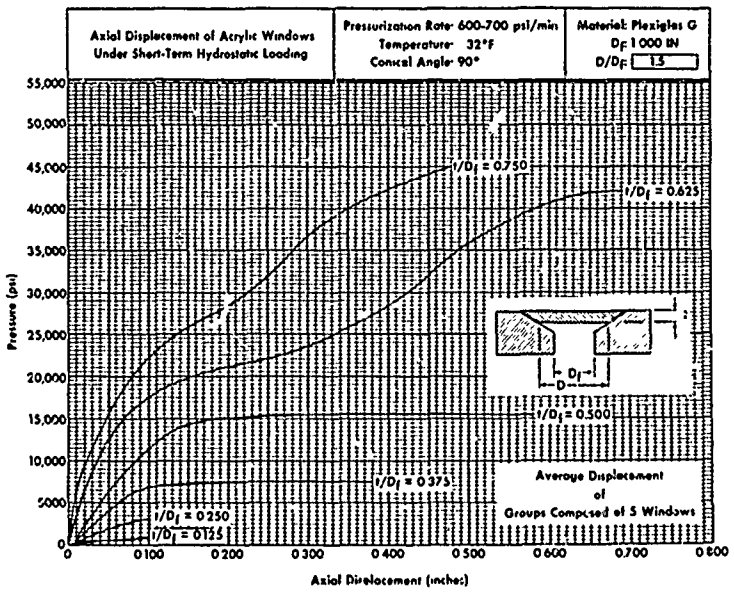


Figure A-13. Effect of short-term hydrostatic loading on axial displacement of 90-degree conical acrylic windows at 32°F ambient temperature;  $D_f = 1.000$  inch,  $D/D_f = 1.500$ .

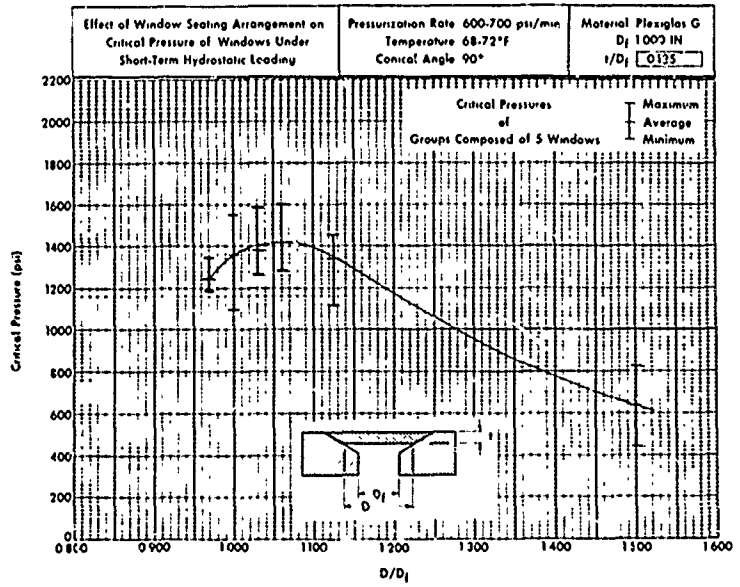


Figure A-14. Effect of seating arrangement on critical pressure of 90-degree conical acrylic windows under short-term hydrostatic loading at 70°F ambient temperature;  $D_f = 1.000$  inch,  $t/D_f = 0.125$ .

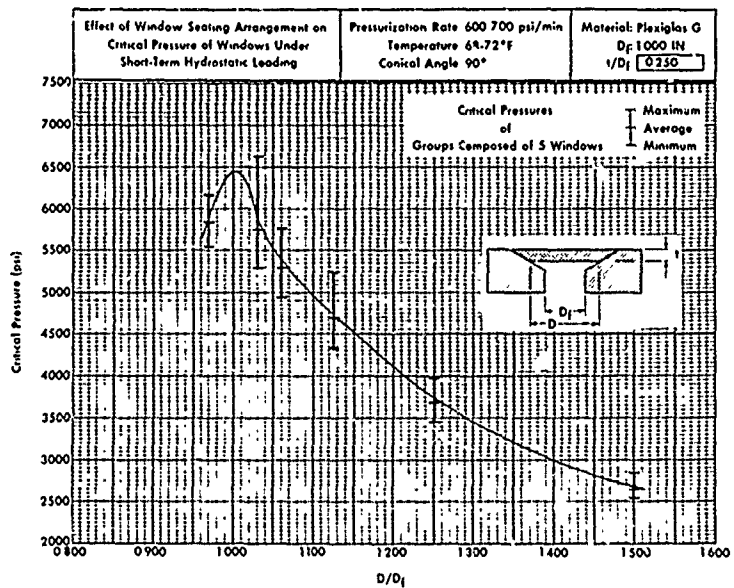


Figure A-15. Effect of seating arrangement on critical pressure of 90-degree conical acrylic windows under short-term hydrostatic loading at 70°F ambient temperature;  $D_f = 1.000$  inch,  $t/D_f = 0.250$ .

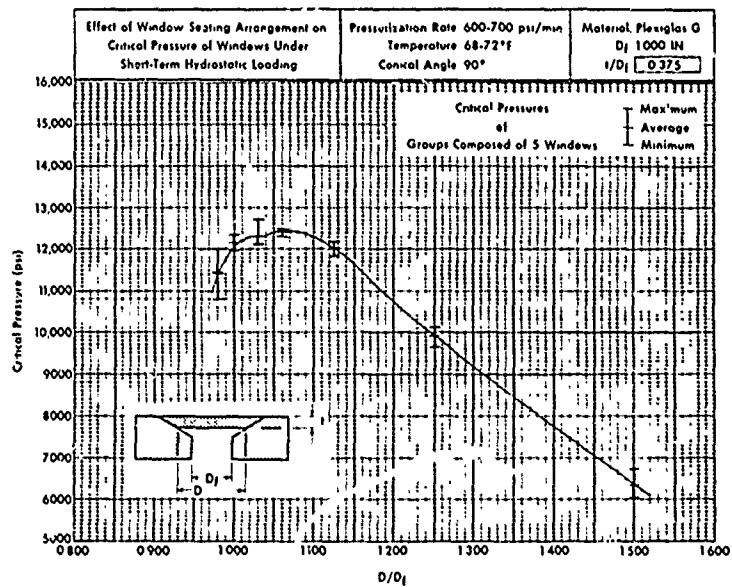


Figure A-16. Effect of seating arrangement on critical pressure of 90 degree conical windows under short-term hydrostatic loading at 70°F ambient temperature;  $D_f = 1.000$  inch,  $t/D_f = 0.375$ .

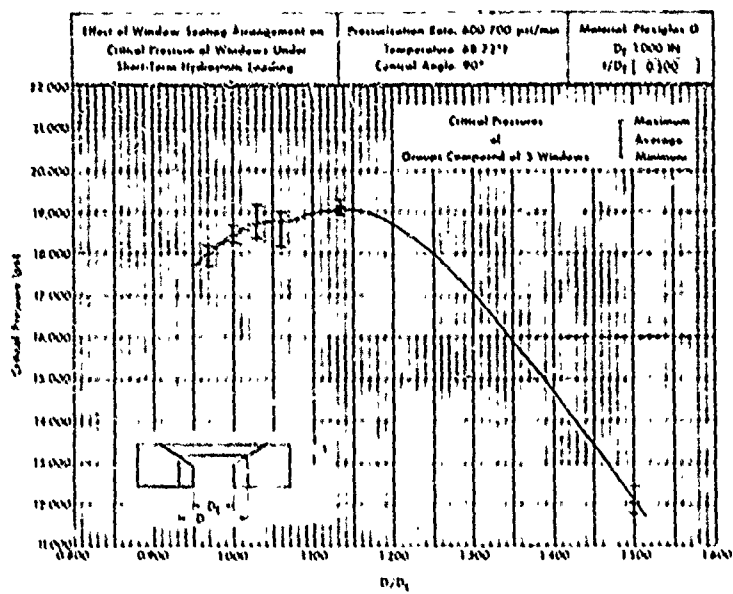


Figure A-17. Effect of seating arrangement on critical pressure of 90-degree conical acrylic windows under short-term hydrostatic loading at 70°F ambient temperature;  $D_f = 1.000$  inch,  $t/D_f = 0.500$ .

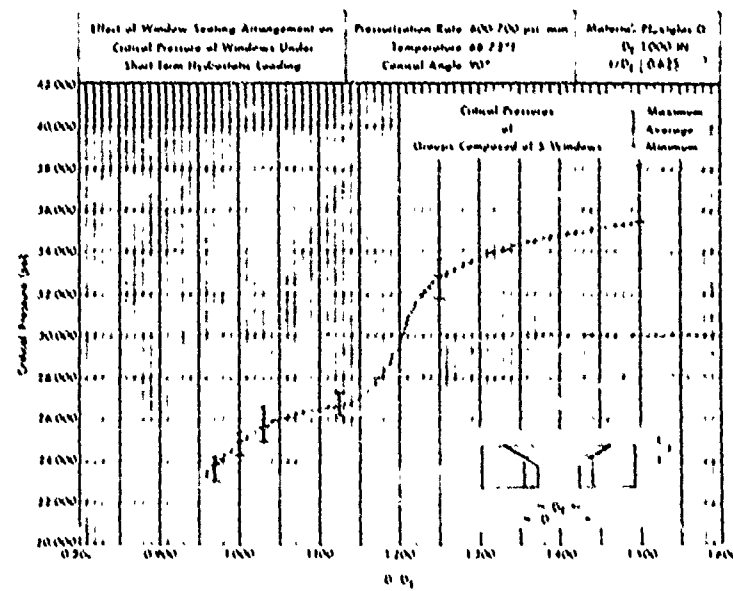


Figure A-18. Effect of seating arrangement on critical pressure of 90-degree conical acrylic windows under short-term hydrostatic loading at 70°F ambient temperature,  $D_f = 1.000$  inch,  $t/D_f = 0.625$ .

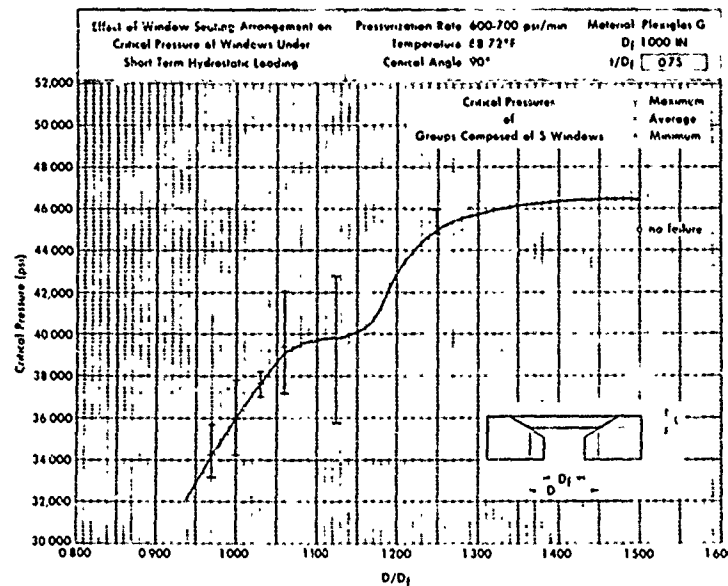


Figure A-19. Effect of seating arrangement on critical pressure of 90-degree conical acrylic windows under short-term hydrostatic loading at 70°F ambient temperature; D<sub>f</sub> = 1.000 inch, t/D<sub>f</sub> = 0.750.

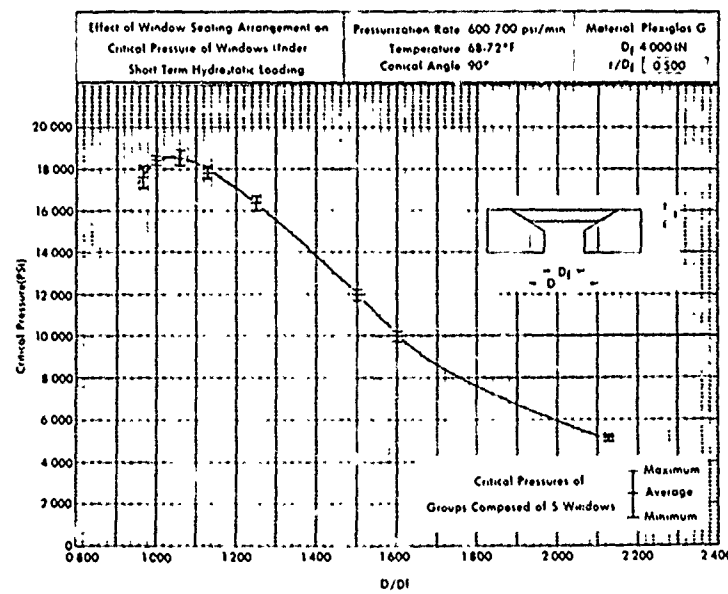


Figure A-20. Effect of seating arrangement on critical pressure of 90-degree conical acrylic windows under short-term hydrostatic loading at 70°F ambient temperature; D<sub>f</sub> = 4.000 inches, t/D<sub>f</sub> = 0.500.

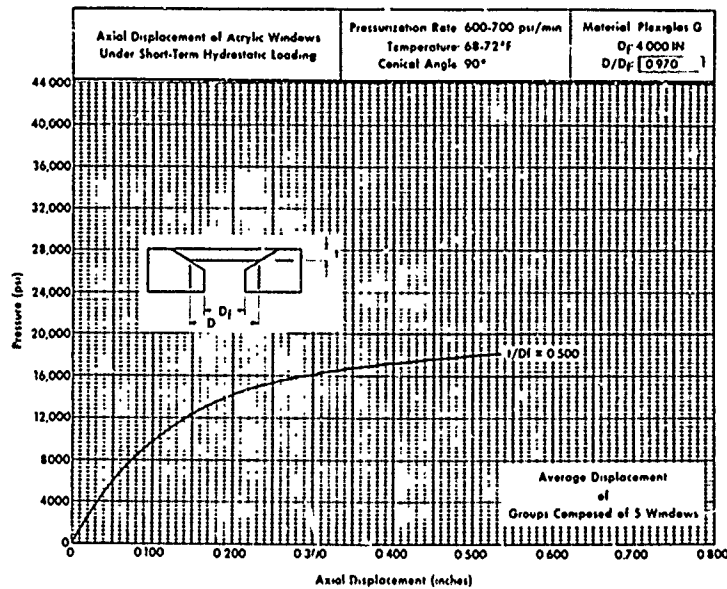


Figure A-21. Effect of short-term hydrostatic loading on axial displacement of 90-degree conical acrylic windows at 70°F ambient temperature;  $D_f = 4.000$  inches,  $t/D_f = 0.500$ ,  $D/D_f = 0.970$ .

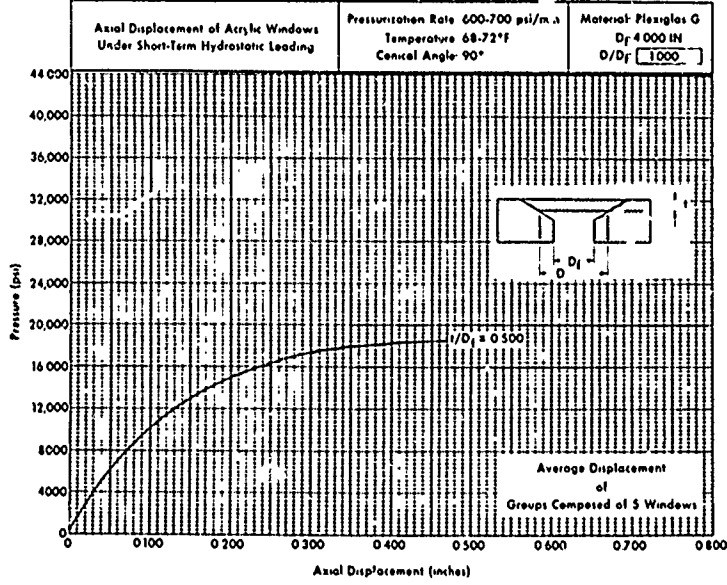


Figure A-22. Effect of short-term hydrostatic loading on axial displacement of 90-degree conical acrylic windows at 70°F ambient temperature;  $D_f = 4.000$  inches,  $t/D_f = 0.500$ ,  $D/D_f = 1.000$ .

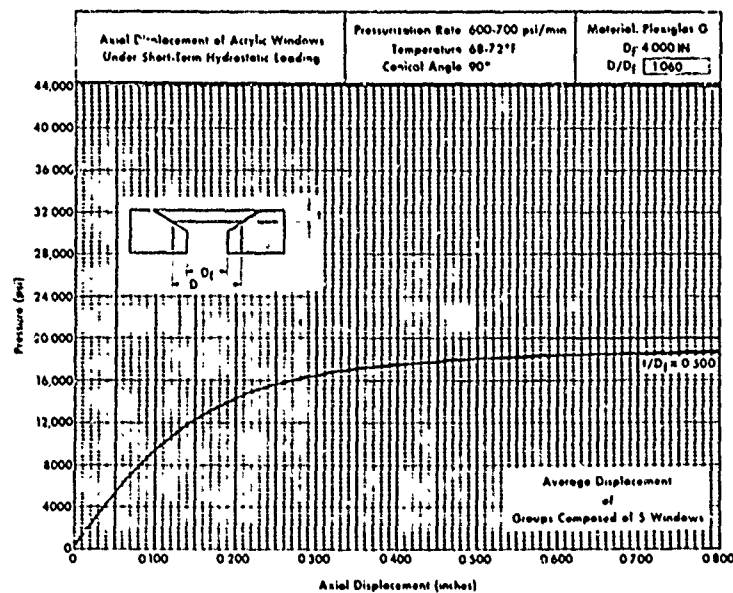


Figure A-23. Effect of short-term hydrostatic loading on axial displacement of 90-degree conical acrylic windows at 70°F ambient temperature;  $D_f = 4.000$  inches,  $t/D_f = 0.500$ ,  $D/D_f = 1.060$ .

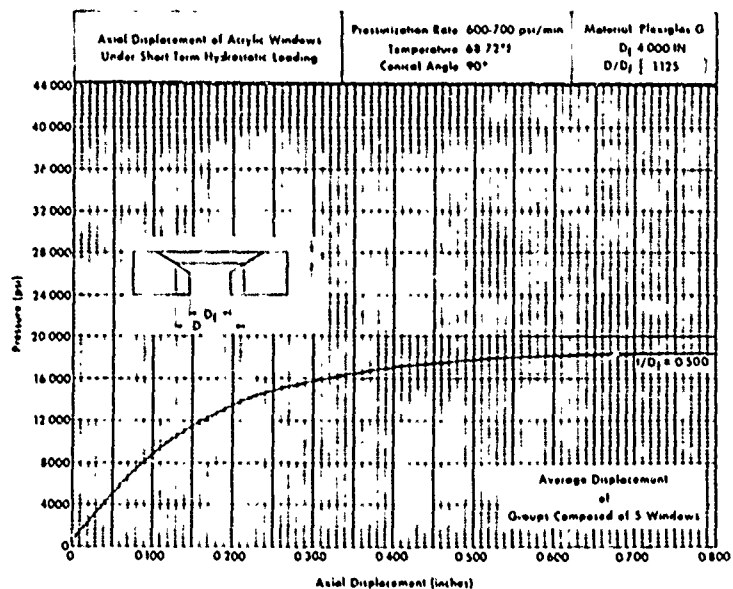


Figure A-24. Effect of short-term hydrostatic loading on axial displacement of 90-degree conical acrylic windows at 70°F ambient temperature;  $D_f = 4.000$  inches,  $t/D_f = 0.500$ ,  $D/D_f = 1.125$ .

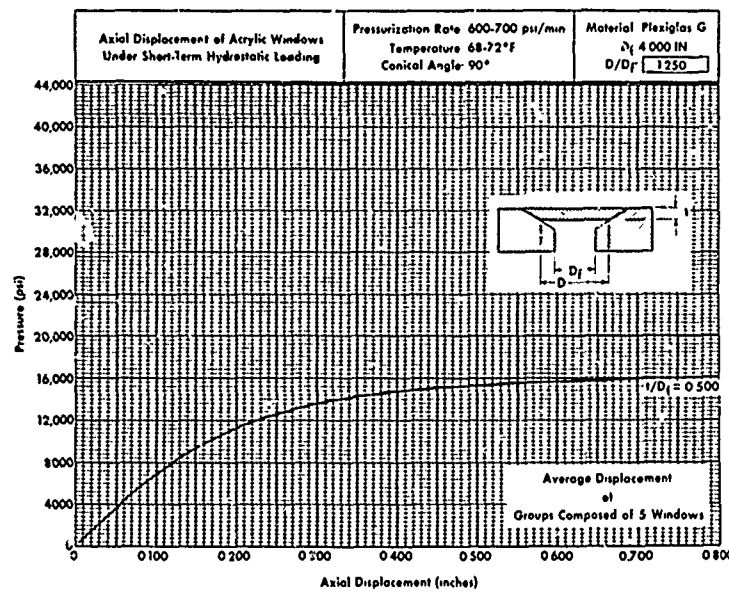


Figure A-25. Effect of short-term hydrostatic loading on axial displacement of 90-degree conical acrylic windows at 70°F ambient temperature;  $D_f = 4.000$  inches,  $t/D_f = 0.500$ ,  $D/D_f = 1.250$ .

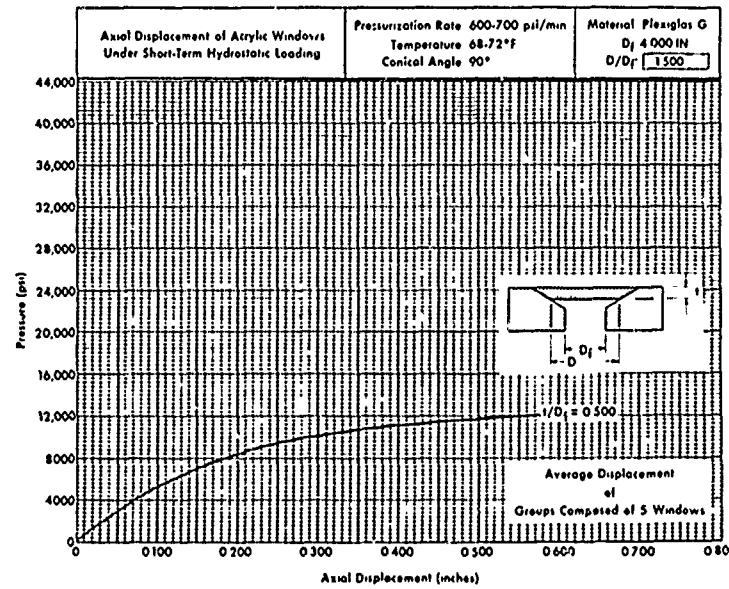


Figure A-26. Effect of short-term hydrostatic loading on axial displacement of 90-degree conical acrylic windows at 70°F ambient temperature;  $D_f = 4.000$  inches,  $t/D_f = 0.500$ ,  $D/D_f = 1.500$ .

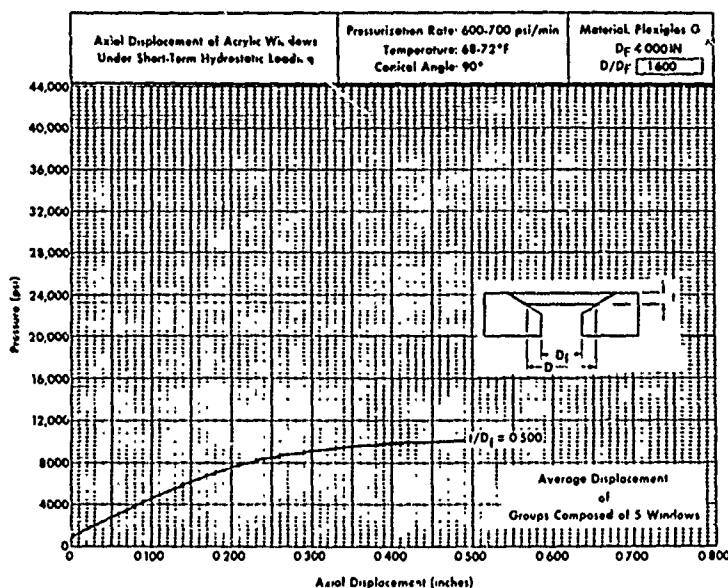


Figure A-27. Effect of short-term hydrostatic loading on axial displacement of 90-degree conical acrylic windows at 70°F ambient temperature;  $D_f = 4.000$  inches,  $t/D_f = 0.500$ ,  $D/D_f = 1.600$ .

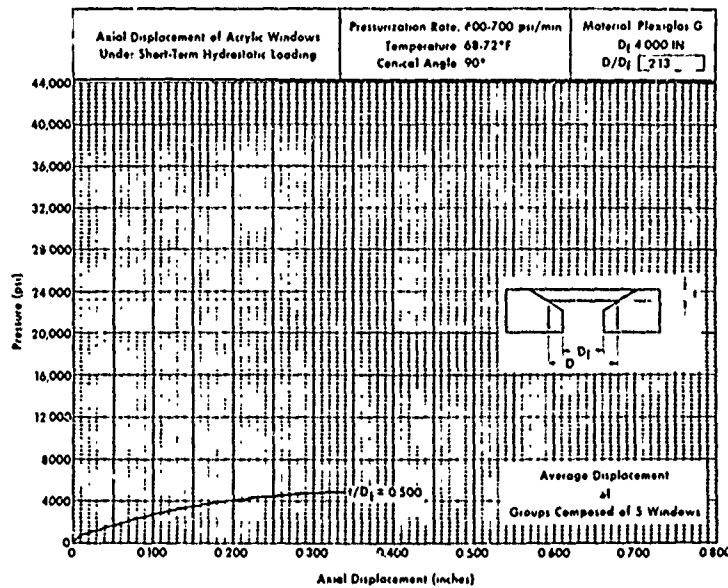


Figure A-28. Effect of short-term hydrostatic loading on axial displacement of 90-degree conical acrylic windows at 70°F ambient temperature;  $D_f = 4.000$  inches,  $t/D_f = 0.500$ ,  $D/D_f = 2.130$ .

## Appendix B

### APPLICATION OF EXPERIMENTAL DATA TO DESIGN OF PRESSURE-RESISTANT WINDOWS

#### BACKGROUND

Conical frustum acrylic plastic windows have been utilized in submersibles, personnel transfer capsules, deck decompression chambers, and deep ocean simulators since they were introduced to such applications by Professor Auguste Piccard through his pioneering FNRS-2 submersible in 1939. Considerable experimental and analytical data have been amassed over the years describing the effects of conical angle and thickness-to-diameter ratio ( $t/D$ ) on the critical pressure, deformation, and axial displacement of such windows under hydrostatic loadings of different durations. Although this information is sufficient for design of safe conical acrylic windows in the 0-to-20,000-psi operational pressure range, it is insufficient to permit maximization of the windows' short-term critical pressure potential through variation in the window seating inside the window containment flange.

That the relationship between the minor diameter of the window ( $D$ ) and that of the flange ( $D_f$ ) affects the critical pressure of the conical acrylic window has been known for a long time<sup>14</sup> but data were not available to permit quantifying this effect. This is not to imply that specific  $D/D_f$  ratios were not recommended for design of windows. Recommendations have been made in the past on choice of proper  $D/D_f$  ratios for different operational pressures, but those recommendations were aimed only at increasing the static and cyclic fatigue life rather than short-term strength of windows. Now that the experimental data on the relationship between short-term critical pressure and  $D/D_f$  ratio are available, it is possible also to specify  $D/D_f$  ratios that will substantially increase the short-term critical pressure that is so important during occurrence of transient depth increases for submersibles or pressure surges inside of deep ocean simulators.

#### DISCUSSION

Since this experimental study has shown (Figure 17) that raising  $D/D_f$  ratios over 1.000 (which in all the NCEL window studies is considered the benchmark ratio) is *never harmful*, and for  $t/D > 0.300$  increasing the ratio is beneficial in raising of short-term critical pressure potential, the designer may be tempted to make the  $D/D_f$  ratio as high as possible so

that a very high short-term critical pressure may be obtained for the window he is designing. This temptation should be resisted, as there are some drawbacks associated also with unlimited  $D/D_f$  increase.

The drawbacks associated with  $D/D_f$  increase are (1) greater costs for window and flange fabrication and (2) increased weight of the window/flange assembly. The increased cost and weight are results of the increased window and flange sizes for a given  $D_f$ . For example, a 90-degree window with  $t/D = 0.5$  located in a flange with  $D_f = 4.000$  inches increased 50% in thickness when the  $D/D_f$  ratio and accompanying critical pressure potential are increased from 1.000 ( $P_c = 19,000$  psi) to 1.500 ( $P_c = 47,000$  psi). The accompanying change in flange thickness will be anywhere from 50% to 100% depending on its structural design. This increase in weight and cost is not followed by any increase in viewing field, as this is always controlled by  $D_f$ , which remains constant.

For this reason, a detailed trade-off study must be conducted between increase in short-term critical pressure potential on one hand and increase in weight and cost of the structure on the other hand before an intelligent decision can be made on what  $D/D_f$  to select for a given window. However, because such trade-off studies may be too long or too complicated for a window designer hard pressed for an answer, a simple set of design guides has been prepared for his use. These simple design guides will permit the designer to rapidly choose a window-seating arrangement ( $D/D_f$ ) that improves not only the short-term critical pressure potential of the window but also its static and cyclic fatigue life.

## DESIGN GUIDES

The simple design guides developed for the benefit of the window designer rest on two basic observations.  $D/D_f > 1.000$  is desirable to give an axially displacing window radial and axial support to its conical bearing surface so that (1) the window's short-term critical pressure potential is increased for unforeseen temporary overload and (2) static and fatigue life of the window is prolonged by eliminating contact between the sharp corner of the flange and the window's bearing surface during pressurizations of the window to its rated operational depth.

From these two basic observations, two general guidelines can be deduced that become helpful in choosing of  $D/D_f$  ratios:

1. Since every window in service will experience static and cyclic fatigue regardless of the relationship between short-term critical pressure and operational pressure chosen, it behooves the designer to prolong the

fatigue life by choosing such a  $D/D_f$  ratio that the conical bearing of the window *never* extends past the supporting conical flange seat during pressurizations to operational depth (Figure B-1). These  $D/D_f$  ratios are considered to be *minimums* and should be met in all operational window designs. Experimental studies have been already conducted for some selected operational depths (20,000 psi, 10,000 psi, and 5,000 psi) and the minimum  $D/D_f$  ratios have been recommended for providing necessary bearing support to the axially displacing windows. Thus for 90-degree conical windows a  $t/D = 2.0$  and  $D/D_f = 1.25$  are recommended for 20,000 psi,  $t/D = 1.0$  and  $D/D_f = 1.15$  for 10,000 psi, and  $t/D = 0.625$  and  $D/D_f = 1.06$  for 5,000 psi. For pressures less than 5,000 psi, experimentally obtained  $D/D_f$  ratio for static or cyclic fatigue do not exist, but a conservative assumption dictates the use of the same minimum  $D/D_f$  ratio as for 5,000-psi operational pressure.

2. Once the minimum  $D/D_f$  ratios required for containment of window axial displacements under operational pressure have been met, further increase of  $D/D_f$  ratios can be justified only by the desire to improve further the short-term critical pressure potential of the window (Figure B-1). What the limit to the improvement should be is, of course, a matter to be decided by the designer, but an increase of more than 50% is very hard to justify, particularly since the proof pressures to which windows may be subjected never exceed the operational pressure by more than 50%.

## EXAMPLE A

### Problem

Choose the proper  $D/D_f$  ratio for a 90-degree conical acrylic window to be utilized in a deep ocean simulator rated for 5,000-psi operational pressure. The service that the window will see will involve long-term, short-term, and dynamic pressure loadings. Before it is placed into service, the window will be proof-tested to 1.5 times its operational pressure.

### Solution

The *minimum*  $t/D$  ratio required to satisfy the static and cyclic fatigue requirements of 5,000-psi service is 0.625 (see Reference 6). The *minimum*  $D/D_f$  ratio that will provide adequate bearing support for the axial window displacement under 5,000-psi operational pressure is 1.06

Note:  $t/D$  is constant in all cases.  
 $D_f$  is constant in all cases.

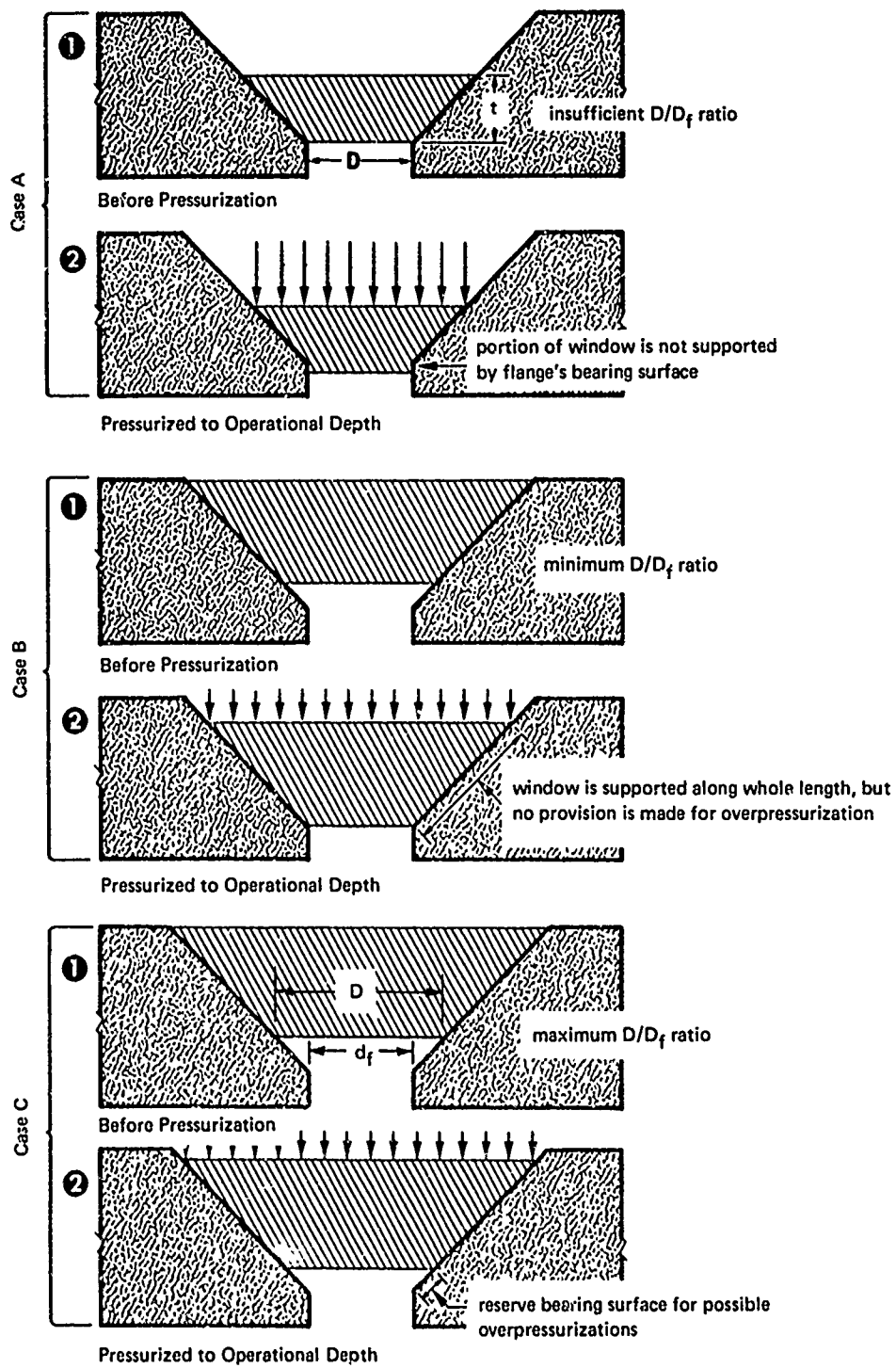


Figure B-1. Effect of  $D/D_f$  ratio on support of window's bearing surface during hydrostatic loading.

(see Reference 6). The *maximum* recommended  $D/D_f$  ratio for the  $t/D = 0.625$  is 1.175 based on planned 50% increase in critical pressure of the window. A  $D/D_f$  of 1.175 was chosen for the window.

## EXAMPLE B

### Problem

Choose the proper  $D/D_f$  ratio for a 90-degree conical window utilized in a research submersible with abyssal depth capability of 36,000 feet. The window will be subjected mostly to cyclic pressure loadings with maximum possible sustained loading of 36-hour durations. Before it is put in service, the window will be proof-tested to 1.25 times its operational pressure.

### Solution

The minimum  $t/D$  ratio required to satisfy the cyclic fatigue requirements of 36,000-foot depth is 2.00 (see Reference 4). The *minimum*  $D/D_f$  ratio that will provide adequate bearing support for the axial window displacement at 36,000-foot depth is 1.25 (see Reference 4). The maximum  $D/D_f$  cannot be determined in this case from curves in Figure 17, since windows of  $t/D = 2.00$  were not tested in the present window-seating study. It would appear however that  $D/D_f = 1.25$  can also serve in this case as the maximum ratio, since observation of curves in Figure 17 leads to the conclusion that  $D/D_f = 1.25$  probably increases the critical pressure more than 24% over  $D/D_f = 1.000$  unless the plastic extrusion pressure is reached sooner. A  $D/D_f$  of 1.250 was chosen for the window.

## EXAMPLE C

### Problem

Choose the proper  $D/D_f$  ratio for a 90-degree conical acrylic window utilized in a submersible for 1,000-foot operational service. The loading on the window will be primarily of cyclic nature with maximum sustained loading of 36-hour duration. Before it is placed into service, the window will be proof-tested to 1.50 times its operational pressure.

## Solution

Since extensive window studies were not conducted previously at 1,000-foot operational depth, specific recommendations do not exist for the selection of  $t/D$  and  $D/D_f$  ratio. Because of this, recourse must be taken to a more arbitrary approach of choosing  $t/D$  ratios. This approach, whatever it lacks in accuracy, makes up through conservatism in application of high safety factors. This approach is based on the observation (Reference 14) that if the short-term critical pressure (Figure 17 at  $D/D_f = 1.00$ ) is divided by a conversion factor of four then the long-term critical pressure is approximately fixed. To insure that the approximately arrived at long-term critical pressure (static fatigue) is valid for (1) repeated pressurization and (2) proof test (overload), it is further divided by a safety factor of two. To summarize, when the short-term critical pressure is divided by a factor of eight, a safe operational pressure has been fixed.

In the case of the 1,000-foot operational depth, it means that a  $t/D$  must be chosen that at  $D/D_f = 1.00$  has a short-term critical pressure of 3,600 psi (that is, 450 psi  $\times$  8). The  $t/D$  corresponding to 3,600-psi short-term critical pressure is found to be 0.200. Since the operational pressure is less than 5,000 psi, the recommended minimum  $D/D_f = 1.06$ . Maximum  $D/D_f = 1.06$  also, since increasing the  $D/D_f$  ratio further does not affect the critical pressure. Thus the final ratios for 1,000-foot operational depth 90-degree conical window are  $t/D = 0.200$  and  $D/D_f = 1.06$ .

Examples A through C refer to applications where the ambient temperature will be in the  $65^{\circ}\text{F}$ -to- $75^{\circ}\text{F}$  range. If the ambient temperature is lower, no corrections need to be made to the chosen  $t/D$  ratios, as the error is on the conservative side and thus acceptable. The situation is slightly different if the ambient temperatures are above the  $65^{\circ}\text{F}$ -to- $75^{\circ}\text{F}$  range. If no corrections were made, the error would be on the unsafe side, resulting in windows with lower safety factors. For this reason, when choosing windows on the basis of their short-term critical pressure (see Example C), effects of higher temperature should be taken into account. Thus Figure 19a, instead of Figure 17, should be used as the basis for determining short-term critical pressure, because Figure 19a takes the effects of temperature into account. Since Figure 19 has only curves for  $D/D_f = 1.00$  and  $D/D_f = 1.50$ , critical pressure values for other  $D/D_f$  ratios must be found by interpolation.

## REFERENCES

1. Naval Civil Engineering Laboratory. Technical Report R-512: Windows for external or internal hydrostatic pressure vessels, pt. 1. Conical acrylic windows under short-term pressure application, by J. D. Stachiw and K. O. Gray. Port Hueneme, Calif., Jan. 1967. (AD 646882)
- 2.———. Technical Report R-527: Windows for external or internal hydrostatic pressure vessels, pt. 2. Flat acrylic windows under short-term pressure application, by J. D. Stachiw, G. M. Dunn, and K. O. Gray. Port Hueneme, Calif., May 1967. (AD 652343)
- 3.———. Technical Report R-631: Windows for external or internal hydrostatic pressure vessels, pt. 3. Critical pressure of acrylic spherical shell windows under short-term pressure application, by J. D. Stachiw and F. W. Brier. Port Hueneme, Calif., June 1969. (AD 689789)
- 4.———. Technical Report R-645: Windows for external or internal hydrostatic pressure vessels, pt. 4. Conical acrylic windows under long-term pressure applications at 20,000 psi, by J. D. Stachiw. Port Hueneme, Calif., Oct. 1969. (AD 697272)
- 5.———. Technical Report R-708: Windows for external or internal hydrostatic pressure vessels, pt. 5. Conical acrylic windows under long-term pressure application of 10,000 psi, by J. D. Stachiw and W. A. Moody. Port Hueneme, Calif., Jan. 1970. (AD 718812)
- 6.———. Technical Report R-747. Windows for external or internal hydrostatic pressure vessels, pt. 6. Conical acrylic windows under long-term pressure application at 5,000 psi, by J. D. Stachiw and K. O. Gray. Port Hueneme, Calif., June 1971. (AD 736594)
- 7.———. Technical Note N-1127: Flat disc acrylic plastic windows for man-rated hyperbaric chambers at the USN Experimental Diving Unit, by J. D. Stachiw. Port Hueneme, Calif., Nov. 1970. (AD 716751)
- 8.———. Technical Report R-676: Development of a spherical acrylic plastic pressure hull for hydrospace application, by J. D. Stachiw. Port Hueneme, Calif., Apr. 1970. (AD 707363)
- 9.———. Technical Note N-1113: The spherical acrylic pressure hull for hydrospace application, pt. 2. Experimental stress evaluation of prototype NEMO capsule, by J. D. Stachiw and K. L. Mack. Port Hueneme, Calif., Oct. 1970. (AD 715772)

10. Naval Civil Engineering Laboratory. Technical Note N-1094: The spherical acrylic pressure hull for hydrospace application, pt. 3. Comparison of experimental and analytical stress evaluations for prototype NEMO capsule, by H. Ottsen. Port Hueneme, Calif., Mar. 1970. (AD 709914)
11. ———. Technical Note N-1134: The spherical acrylic pressure hull for hydrospace application, pt. 4. Cyclic fatigue of NEMO capsule #3, by J. D. Stachiw. Port Hueneme, Calif., Oct. 1970. (AD 715345)
12. ———. Technical Report R-675: Stress analysis of a conical acrylic viewport, by M. R. Snoey and J. E. Crawford. Port Hueneme, Calif., Apr. 1970. (AD 708009)
13. Armed Forces Supply Support Center. Military Handbook 17: Plastics for flight vehicles, pt. 2. Transparent glazing materials. Washington, D. C., Aug. 1961.
14. M. R. Snoey and J. D. Stachiw. "Windows and transparent hulls for man in hydrospace," in a critical look at marine technology; transactions of the 4th annual MTS conference and exhibit, Washington, D. C., July 8-10, 1968. Washington, D. C., Marine Technology Society, 1968, pp. 419-463.